Phytochemistry 69 (2008) 2463–2481

Contents lists available at ScienceDirect

Phytochemistry

journal homepage: www.elsevier.com/locate/phytochem

Non-targeted analysis of spatial metabolite composition in strawberry (*Fragaria* × *ananassa*) flowers

Kati Hanhineva [a,b], Ilana Rogachev [a], Harri Kokko [b], Shira Mintz-Oron [a], Ilya Venger [a], Sirpa Kärenlampi [b], Asaph Aharoni [a,*]

[a] Department of Plant Sciences, Weizmann Institute of Science, P.O. Box 26, Rehovot 76100, Israel
[b] Department of Biosciences, University of Kuopio, P.O. Box 1627, Kuopio 70211, Finland

ARTICLE INFO

Article history:
Received 27 February 2008
Received in revised form 17 July 2008
Available online 4 September 2008

Keywords:
Strawberry (*Fragaria* × *ananassa*)
Rosaceae
Secondary metabolite profiling
Floral metabolites
UPLC-qTOF-MS
Ellagitannin
Proanthocyanidin
Flavonol
Terpenoid
Spermidine

ABSTRACT

Formation of flower organs and the subsequent pollination process require a coordinated spatial and temporal regulation of particular metabolic pathways. In this study a comparison has been made between the metabolite composition of individual flower organs of strawberry (*Fragaria* × *ananassa*) including the petal, sepal, stamen, pistil and the receptacle that gives rise to the strawberry fruit. Non-targeted metabolomics analysis of the semi-polar secondary metabolites by the use of UPLC-qTOF-MS was utilized in order to localize metabolites belonging to various chemical classes (e.g. ellagitannins, proanthocyanidins, flavonols, terpenoids, and spermidine derivatives) to the different flower organs. The vast majority of the tentatively identified metabolites were ellagitannins that accumulated in all five parts of the flower. Several metabolite classes were detected predominantly in certain flower organs, as for example spermidine derivatives were present uniquely in the stamen and pistil, and the proanthocyanidins were almost exclusively detected in the receptacle and sepals. The latter organ was also rich in terpenoids (i.e. triterpenoid and sesquiterpenoid derivatives) whereas phenolic acids and flavonols were the predominant classes of compounds detected in the petals. Furthermore, we observed extensive variation in the accumulation of metabolites from the same class in a single organ, particularly in the case of ellagitannins, and the flavonols quercetin, kaempferol and isorhamnetin. These results allude to spatially-restricted production of secondary metabolite classes and specialized derivatives in flowers that take part in implementing the unique program of individual organs in the floral life cycle.

© 2008 Elsevier Ltd. All rights reserved.

1. Introduction

Flowers are complex structures in angiosperms that serve the purpose of producing the next generation through seed development and dispersal. Floral organs such as sepals, petals, stamens and pistils are structurally and functionally discrete entities responsible for plant reproduction *via* pollen development, attraction of pollinators, fertilization and induction of fruit and seed development. The main role of each organ is well defined and the reproductive process is well described, however the knowledge of the biochemical mechanisms that take part in the reproduction process is still limited (Ingrouille 2002; Palanivelu et al., 2003).

Successful fertilization requires an interplay between the reproductive organs of the flower, namely the female organ (pistil containing one or several carpels enclosing the ovules) and the male organ (stamen consisting of a filament and a pollen-producing anther). Both intricate chemical signaling (Johnson and Preuss, 2002; Palanivelu et al., 2003) and specific protein expression patterns are required for the pollen grain to reach the ovule and successfully fuse with the egg cell (Escobar-Restrepo et al., 2007). This complex cascade has been found to involve certain metabolite groups; for example flavonols are required for pollen viability (Mo et al., 1992; Ylstra et al., 1994), polyamines function as growth regulators (Sood and Nagar, 2004), and specific lipids are essential for the interaction of the pollen with the stigma (Wolters-Arts et al., 1998).

In a large number of flowering plants petals form the most eye-catching part of the flower, and serve to attract pollinators with inviting colors and appealing scent. Anthocyanins are a major class of compounds forming floral pigmentation. The accumulation of anthocyanins is well characterized both at the gene expression and biochemical levels and comprehensive analysis as well as metabolic engineering of the anthocyanin composition of flowers has been reported several times (Moyano et al., 1996; Winkel-Shirley, 2001; Mol et al., 1999; Nielsen et al., 2005). Concomitantly with anthocyanins, flavanones and flavonols are present in petals as anthocyanin co-pigments and contribute to the different shades of flowers (Nielsen et al., 2005; Fukui et al., 2003). The biosynthesis of fragrant volatiles, including terpenoid and phenylpropanoid/

* Corresponding author. Tel.: +972 8 934 3643; fax: +972 8 934 4181.
E-mail address: asaph.aharoni@weizmann.ac.il (A. Aharoni).

0031-9422/$ - see front matter © 2008 Elsevier Ltd. All rights reserved.
doi:10.1016/j.phytochem.2008.07.009

benzenoid compounds as well as aliphatic esters, amines (indols) and thiols, occurs predominantly in the petal tissues; their emission is under temporal regulation and occurs when pollinators are active (Schuurink et al., 2006; van Schie et al., 2006). The color and fragrance provide the aesthetic properties to ornamentals and cut flowers, and bioengineering approaches are on-going for commercial purposes (Pichersky and Dudareva, 2007). The main role of sepals is to provide protection to the flower bud during the early development of the flower (Ingrouille, 2001). Sepals are usually the only green part of the flower, and are responsible for photosynthesis and carbohydrate production for the developing flower (Kwak et al., 2007).

Floral development offers an excellent model for studying organogenesis including specification of floral organ identities and the formation of inflorescence (Weigel, 1998). Floral mutants show homeotic phenotypes with one floral organ replaced by another, and detailed study of these mutants has led to the definition of the widely accepted ABC model of floral organ identity. In the model, the genes are classified into three different sets, each required for the organ specification in different floral regions (Coen and Meyerowitz, 1991; van der Krol and Chua, 1993; Wellmer et al., 2004). Several thousands of genes are expressed during floral development, the majority of which encode transcription factors or other proteins participating in the regulation of floral organogenesis (Hu et al., 2003; Wellmer et al., 2006). Genome-wide microarray analysis of Arabidopsis flowers at different developmental stages provided information on differentially expressed genes in between floral genes (Wellmer et al., 2006). A relatively high number of genes associated with developmental pathways have been localized to specific floral organs, mostly in the reproductive part of the flower (e.g. stamen and carpel) but genes predominantly expressed in sepals or petals have also been detected (Wellmer et al., 2006). Analysis of the floral transcriptome of *Gerbera hybrida* allowed the identification of several abundantly expressed tissue-specific genes that are associated with transcriptional regulation, cell structure, signal transduction, disease response, secondary metabolism (Laitinen et al., 2005).

Up to date, despite the wide application of metabolomics in plant research, relatively few studies have been performed on the differences in metabolite composition between floral organs. These reports either described non-targeted analysis of flowers as a whole (Li et al., 2006; Spitaler et al., 2006) or were focused on specific metabolite classes such as flavonoids (Nielsen et al., 2005; Lai et al., 2007) or phenolic acids (Clifford et al., 2006; Lai et al., 2007). Thus, an extensive metabolite profile of individual organs composing a flower of a particular plant species has not been described previously. As transcriptomics does not indicate the actual biochemical status of the tissues, metabolite profiling is fundamental for a comprehensive understanding of the physiology of floral organs.

The garden strawberry (*Fragaria* × *ananassa*) belongs to the subfamily Rosoideae of the Rosaceae family. Rosoideae species, particularly those belonging to the genera *Rosa, Rubus and Fragaria* are known to contain versatile secondary metabolism, being especially rich in ellagitannins (Okuda et al., 1992; Kähkönen et al., 2001). Because of the versatile ellagitannin composition, plants of the Rosaceae family are interesting also from the medicinal point of view. Flowers of *Rosa rugosa* and *Rosa chinensis* have been used in traditional Chinese medicine for treating disorders including trauma, diarrhoea and blood disorders, and the main pharmaceutical effect is believed to be due to ellagitannins (Cai et al., 2005; Hashidoko, 1996). In addition, ellagitannins have been shown *in vitro* to have antioxidative (Mullen et al., 2002) and anticarcinogenic (Seeram et al., 2007) activities. Strawberry is the most widely cultivated member of the Rosoideae and fairly extensive information is available on the chemical composition of its fruit (Aaby et al., 2007; Määttä-Riihinen et al., 2004; Aharoni et al., 2002). In this study, we used a LC–MS based metabolomics approach for investigating the methanol extractable compounds of five strawberry flower organs namely, petals, sepals, stamens, pistils and the receptacle (Fig. 1A). Since the base of the flower, the receptacle, gives rise to the fruit, this work is complementary to the previous work of Aharoni et al. (2002) in which a non-targeted metabolomics approach was used to profile later stages of strawberry receptacle development.

2. Results and discussion

2.1. Identification of metabolites in the strawberry floral organs

To assess the differences in the composition of metabolites of strawberry floral organs, a non-targeted metabolite profiling of extracts derived from dissected petal, sepal, stamen, pistil and receptacle samples was conducted. Methanol-soluble constituents from the various organs were analysed by a high resolution UPLC-PDA-qTOF-MS. Principal component analysis (PCA) demonstrated that striking differences exist between the metabolic profiles of different organs (Fig. 1B). Interestingly, the most distinct profiles were those obtained from extracts of sepals that represent the most outer whorl of the flower. This observation might be explained by the relative structural similarity of sepals to leaves and vegetative, photosynthetic organs. Following the identification process (see experimental), we assigned 109 chromatographic peaks a tentative identification and sorted them to specific metabolite classes (Table 1). The assigned peaks observed in the total ion chromatograms (TIC, negative ESI) are marked for each organ in Fig. 2 and the metabolite name corresponding to each number is presented in Table 1.

2.2. Identification of phenolics, the major class of secondary metabolites detected in strawberry floral organs

Secondary metabolites belonging to the phenolic class have been frequently reported from strawberry fruit and leaves (Aaby et al., 2007; Hukkanen et al., 2007; Määttä-Riihinen et al., 2004). Precursors for most phenolic metabolites are the phenolic acids, that are commonly reported in metabolite profiling studies of plant material; often conjugated with sugars (Mattila and Kumpulainen, 2002; Määttä et al., 2003). In this study, for all the phenolic acids one main fragment ion was present in the negative ionization mode after the loss of a sugar unit, i.e., the charged aglycone, but in the positive mode also a loss of water ($[M+H-18]^+$) and a sodium adduct ion ($[M+23]^+$) were observed in several cases, for example for caffeic acid hexose (**10**) and coumaric acid hexose (**21**). The MS/MS fragments of the aglycones were compared with the fragments obtained from the corresponding phenolic acid standards to verify their identification.

Flavonoids are frequently detected in reversed-phase LC–MS, especially when accompanied by PDA detection, and have been studied also in strawberry fruit (Aaby et al., 2007; Määttä-Riihinen et al., 2004) and leaves (Hukkanen et al., 2007). *In planta* flavonoids are usually substituted with one or several sugars, and/or are acylated by acid moieties. The quasi-molecular ion and the loss of substituents were recognized in the MS spectrum, as exemplified by the in source fragmentation of kaempferol pentose-hexose-glucuronide (**20**; see Fig. 3A). The reconstituted ion chromatograms of each mass spectrum showed that all the fragments originated from the same compound (Fig. 3B).

Isorhamnetin is a methylated derivative of quercetin and has been reported to occur in *Rubus* species (*Rosaceae* family members) but not in strawberry (Määttä-Riihinen et al., 2004). In this study MS/MS analysis of four compounds (**58, 69, 71** and **83**) suggested

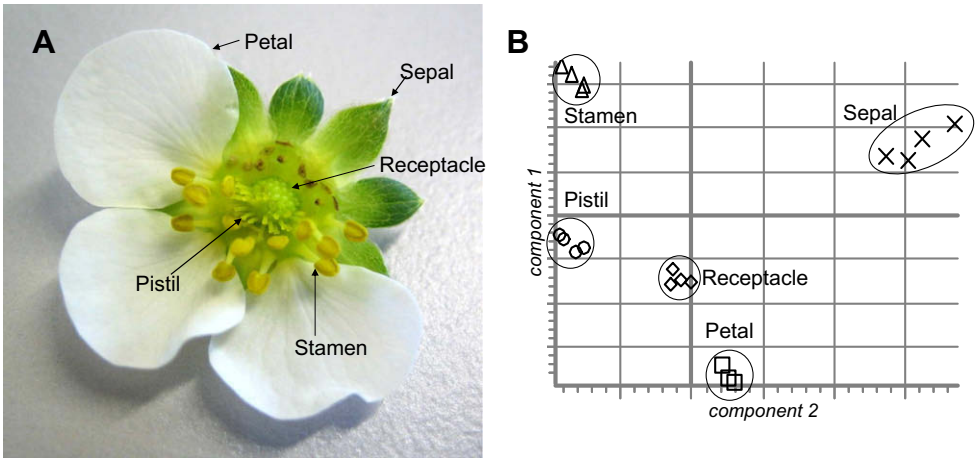

Fig. 1. Strawberry floral organs analyzed for metabolite composition. (A) Strawberry flower at the anthesis stage. Organs analyzed in this study are depicted; (B) principal component analysis of the metabolite markers obtained from the separated floral organs (performed in the Marker Lynx software on peak areas with Pareto scaling). $n = 4$ apart from petals ($n = 3$).

the structure of isorhamnetin derivatives based on the ES(−) fragment ions: *m/z* 315.0501 (the aglycon ion) and subsequent loss of methyl from the methoxy group (−15 Da). The MS/MS analysis of isorhamnetin standard resulted in fragments *m/z* 300.027, 283.024, 271.024, 255.029, 243.0288, 227.035, 215.0340, 199.0397 and 151.003 in ES(−), whereas ES(+) fragments were *m/z* 302.044, 285.042, 273.041, 245.046, 229.05, 217.0514, 203.036 and 153.020. Several of these fragments were observed also in the suggested isorhamnetin derivatives in both ionization modes (Table 1). The elemental composition suggested for the compound corresponding to the ion *m/z* 315.0501 was $C_{16}H_{12}O_7$ (formula of isorhamnetin, to distinguish from methylated ellagic acid) which further supports the identification. The compound **19** showed the loss of three sugar units from a *m/z* 317.066 aglycon in ES(+), but the aglycon did not result in isorhamnetin-like fragmentation and thus remained unknown.

Formation of flavonol aglycon radical ions in MS/MS with high collision energies is a well known phenomenon (Cuyckens and Claeys, 2005; Petsalo et al., 2006). It was observed also in this study, as the aglycon ions of quercetin malonylhexose (**75**) and quercetin glucoside (**72**) gave in addition to the deprotonated aglycon ion (*m/z* 301.0345) a mass signal at *m/z* 300.0258 (Fig. 3C). The radical ion formation was detected also for derivatives of isorhamnetin visible as the fragment of *m/z* 314.04 in the negative MS/MS (**58, 69, 71**). The loss of the methyl group from *m/z* 314.04 formed the fragment at 299.02 amu. The aglycon radical formation phenomenon was not observed in the case of kaempferol fragmentation.

Proanthocyanidins were detected by their characteristic fragmentation of flavan oligomers (loss of catechin units, 288 amu) and by UV/visible spectrum exhibiting λ_{max} at 278 nm (Nunez et al., 2006; Gu et al., 2003). In addition to procyanidin polymers also propelargonidins have been reported in strawberry fruit (Gu et al., 2003). The latter were detectable in this study in flowers as well. They were mainly detected in sepals, in four main peaks (**23, 25, 29, 33**) and identified based on elemental composition calculation and fragmentation patterns that contained the diagnostic ions of *m/z* 435, 407, 289, 271 and 125 amu in ES(−) (Gu et al., 2003).

Ellagitannins are polyphenolic compounds with a sugar core exhibiting typical features in LC–MS analysis; loss of gallic acid moieties (152 or 170 amu), loss of an hexahydroxydiphenyl unit (HHDP; 302 amu) and a sugar unit (162 or 180 amu), repetitive loss of water molecules and tendency to form double charged ions (Okuda et al., 1992; Mullen et al., 2003; Hukkanen et al., 2007). Occurrence of one or several of the diagnostic ions of the ellagitannin backbone (listed in Fig. 4A) is typically detected in the MS spectrum. UV/visible spectrum shows λ_{max} at the range of 270 to 280 nm, and the intensity of the spectrum reflects the amount of free galloyl moieties present in the molecule; the more free galloyl moieties present, the sharper is the spectrum profile, and if all the galloyl units are interlinked, the spectrum is merely a 'slope' (Fig. 4B). A distinctive characteristic in this compound group was the qualitative abundance; as many as 41 peaks were proposed to represent ellagitannins or their galloylglucose precursors. The abundance of the compounds in this metabolite group is also visible in the TIC that is extremely rich in the elution region of ellagitannins (R_t 2–12 min), especially in stamen, pistil and receptacle samples (Fig. 2C–E). Approximately half of those peaks could be assigned as a previously characterized ellagitannin or precursor (Table 1). The trivial names of different ellagitannin isomers are based on their stereoisoforms. In this study the compounds are however abbreviated according to the composition of the molecule, such as digalloyl-HHDP-glucose (**46**) or bis-HHDP-glucose (**5**, **11**). The two stereoisoforms of the galloyl-bis-HHDP-glucose (casuarictin, peak **48** and potentillin, peak **54**) are an exception; they have been reported previously in strawberry leaves and are identifiable by the elution order in reversed-phase LC (Hukkanen et al., 2007). While carrying out an elemental composition analysis for several of the unidentified peaks exhibiting the ellagitannin characteristics in their spectra and using the resulting formulae to search for a putative metabolite identity we obtained only identifications (or hits) that correspond to ellagitannins. Although we cannot rule out the possibility that some forms of ellagitannins result from fragmentation during extraction, the fact that qualitative differences in ellagitannin peaks are observed between different flower organs extracts supports the natural presence of these forms. However, targeted analysis accompanied by additional purification and optimized chromatographic conditions together with additional MS/MS and NMR analysis is needed to further clarify the ellagitannin repertoire of strawberry flower organs.

2.3. Spermidine and terpenoid derivatives putatively identified in strawberry floral organs

Metabolite profiling of the floral tissues revealed a set of metabolites, derivatives of spermidines and terpenoids that have not been reported previously in strawberry. Spermidine derivatives were detected as acylated in different combinations of coumaric,

Table 1
Metabolites putatively identified by UPLC-qTOF-MS and MS/MS analysis in strawberry flowers

Peak no.	R_t(min)	*m/z* ES(−)	*m/z* ES(+)	λ_{max} (nm)	Tentative structural assignment	Molecular formula	MM	Δmass (ppm)	Ref.
1	1.15	**481.0614 [M−H]$^-$, 300.9970 [M−H−Hex]$^-$, 421.0421, 275.0201, 249.0417**		Slope	HHDP-glucose	$C_{20}H_{18}O_{14}$	482.0697	−0.83	
2	1.23	**331.0629 [M−H]$^-$, 169.0132 [M−H−Hex]$^-$, 271.0460, 211.0223, 151.0032**		276	Galloylglucose	$C_{13}H_{16}O_{10}$	332.0743	−10.87	Aharoni et al. (2002)
3	1.43	**343.0670 [M−H]$^-$, 191.0483 [M−H−Gall]$^-$,** 687.1390 [2M−H]$^-$		270	Galloylquinic acid	$C_{14}H_{16}O_{10}$	344.0743	1.46	
4	1.97		166.0876 [M+H]$^+$, 120.0805	n.a.	Phenylalanine (s)	$C_9H_{11}NO_2$	165.0790	4.82	Aharoni et al. (2002)
5	2.38	**783.0638 [M−H]$^-$, 481.0608 [M−H−HHDP]$^-$, 300.9982 [M−H−HHDP−Hex]$^-$,** 275.0174, 391.0271 [M−2H]$^{2-}$		Slope	Bis-HHDP-glucose	$C_{34}H_{24}O_{22}$	784.0759	−5.49	Aaby et al. (2007)
6	3.30	**633.0735 [M−H]$^-$, 463.0489 [M−H−Gallic acid]$^-$, 300.9984 [M−H−Gallic acid−Hex]$^-$, 481.0612, 275.0154**		276	Galloyl-HHDP-glucose	$C_{27}H_{22}O_{18}$	634.0806	1.11	Aaby et al. (2007)
7	3.42	497.0578 [M−H]$^-$, 479.0456 [M−H−H_2O]$^-$, 300.9981 [M−H−H_2O−178]$^-$	499.0720 [M+H]$^+$, 481.0622 [M+H−H_2O]$^+$, 463.0515 [M+H−2(H_2O)]$^+$, 337.0203 [M+H−Hex]$^+$	n.a.	Unknown ellagitannin	$C_{20}H_{18}O_{15}$	498.0646	2.21	
8	3.62		205.0981 [M+H]$^+$, 188.0699	n.a.	Tryptophan (s)	$C_{11}H_{12}N_2O_2$	204.0899	1.95	Aharoni et al. (2002)
9	3.67	**495.0792 [M−H]$^-$, 343.0650 [M−H−Gall]$^-$, 191.0420 [M−H−Gall−Gall]$^-$, 325.0541, 169.0153**		n.a.	Digalloylquinic acid	$C_{21}H_{20}O_{14}$	496.0853	3.43	
10	3.73	**341.0860 [M−H]$^-$, 179.0360 [M−H−Hex]$^-$, 161.0248**	365.0851 [M+Na]$^+$	sh-324	Caffeic acid hexose (s)	$C_{15}H_{18}O_9$	342.0951	−3.81	Määttä-Riihinen et al. (2004)
11	3.81	**783.0644 [M−H]$^-$, 481.0606 [M−H−HHDP]$^-$, 300.9982 [M−H−HHDP−Hex]$^-$**		Slope	Bis-HHDP-glucose	$C_{34}H_{24}O_{22}$	784.0759	−4.73	Aaby et al. (2007)
12	4.21	**577.1332 [M−H]$^-$, 425.0882 [M−H−152]$^-$, 407.0788 [M−H−170]$^-$, 289.0703 [M−H−Cat]$^-$, 245.0244, 125.0244, 451.1044**	579.1476 [M+H]$^+$	278	Procyanidin dimer	$C_{30}H_{26}O_{12}$	578.1424	−6.93	Aaby et al. (2007), Määttä-Riihinen et al. (2004), Hukkanen et al. (2007) and Ishimaru et al. (1995)
13	4.30	**785.1811 [M−H]$^-$, 623.1254 [M−H−Hex]$^-$, 447.0916 [M−H−Hex−Gln]$^-$, 285.0392 [M−H−Hex−Gln−Hex]$^-$, 665.1325, 337.0815**		264, 345	Kaempferol di-hexose glucuronide	$C_{33}H_{38}O_{22}$	786.1855	4.46	
14	4.43	**483.0754 [M−H]$^-$, 331.0621 [M−H−Gall]$^-$, 313.0573 [M−H−Gall−H_2O]$^-$, 271.0443 [M−H−Gall−60]$^-$, 169.0138 [M−H−Gall−Hex]$^-$**		276	Digalloylglucose	$C_{20}H_{20}O_{14}$	484.0853	−4.35	
15	4.48	**865.1962 [M−H]$^-$, 577.1341 [M−H−Cat]$^-$, 287.0548 [M−H−Cat−290]$^-$, 739.1658, 695.1350, 451.0986, 425.0854**		278	Procyanidin trimer	$C_{45}H_{38}O_{18}$	866.2058	−2.08	Aaby et al. (2007)
16	4.63	**353.0866 [M−H]$^-$, 191.0560 [M−H−Caff]$^-$**		sh-323	Chlorogenic acid (s)	$C_{16}H_{18}O_9$	354.0951	−1.98	
17	4.66	**289.0691 [M−H]$^-$, 245.0809, 221.0805, 203.0693, 161.0608, 151.0387, 125.0236, 123.0439, 109.0281**	291.0869 [M+H]$^+$	279	Catechin[a]	$C_{15}H_{14}O_6$	290.0790	−7.26	Aharoni et al. (2002), Aaby et al. (2007), Määttä-Riihinen et al. (2004), Ishimaru et al. (1995) and Seeram et al. (2006)
18	4.86	**865.2006 [M−H]$^-$, 739.1659, 695.1385, 577.1367, 425.0883, 287.0572**	867.2136 [M+H]$^+$	278	Procyanidin trimer	$C_{45}H_{38}O_{18}$	866.2058	3.01	Aaby et al. (2007)
19	4.92	**801.2105 [M−H]$^-$, 639.1568, 476.0719, 314.0517**	803.2259 [M+H]$^+$, 641.1703 [M+H−Hex]$^+$, 479.1184 [M+H−Soph]$^+$, 317.066 [M+H−Soph−Hex]$^+$	n.a.	Unknown				
20	4.96	755.1652 [M−H]$^-$	**757.1812 [M+H]$^+$,625.1392 [M+H−Pent]$^+$,463.0864 [M+H−Pent−Hex]$^+$, 449.1089 [M+H−Pent−Gln]$^+$, 287.056 [M+H−Pent−Gln−Hex]$^+$**	264, 345	Kaempferol pentose hexose glucuronide	$C_{32}H_{36}O_{21}$	756.1749	4.62	

21	5.02	**325.0895 [M−H]$^-$, 163.0402 [M−H−Hex]$^-$, 145.0295 [M−H−Hex−H_2O]$^-$**	327.1073 [M+H]$^+$, 349.0902 [M+Na]$^+$, 165.0545 [M+H−Hex]$^+$, 147.0436 [M+H−Hex−H_2O]$^+$	314	Coumaric acid hexose (s)	$C_{15}H_{18}O_8$	326.1002	−8.61	Aaby et al. (2007), Määttä-Riihinen et al. (2004), Hukkanen et al. (2007) and Seeram et al. (2006)
22	5.03	**633.0706 [M−H]$^-$, 300.9976 [M−H−332]$^-$, 463.0509, 275.0218**	635.0903 [M+H]$^+$, 483.078 [M+H–Gall]$^+$, 321.0256 [M+H–Gall–Hex]$^+$, 303.0144 [M+H–Gall–Hex–H_2O]$^+$, 617.0795 [M+H–H_2O]$^+$, 465.0673 [M+H–H_2O–Gall]$^+$, 447.055 [M+H−H_2O−Gall−H_2O]$^+$, 429.0471 [M+H−H_2O−Gall−2(H_2O)]$^+$	277	Galloyl-HHDP-glucose	$C_{27}H_{22}O_{18}$	634.0806	−3.48	Aaby et al. (2007)
23	5.12	**561.1413 [M−H]$^-$, 289.0691 [M−H−Afz]$^-$, 245.0871**		277	Propelargonidin dimer	$C_{30}H_{26}O_{11}$	562.1475	2.85	Gu et al. (2003)
24	5.23	**625.1419 [M−H]$^-$, 463.09888, 301.0377**	**627.1579 [M+H]$^+$, 465.1012 [M+H−Hex]$^+$, 303.0485 [M+H−2Hex]$^+$**	n.a.	Quercetin di-hexose	$C_{27}H_{30}O_{17}$	626.1483	−10.24	
25	5.44	**849.2055 [M–H]$^-$, 559.1221 [M–H–290]$^-$, 723.1591, 679.1462, 433.0960, 407.0712, 289.0724, 271.0696, 125.0215**		276	Propelargonidin trimer	$C_{45}H_{38}O_{17}$	850.2109	2.83	Gu et al. (2003)
26	5.46	965.0887 [M−H]$^-$, 783.0718 [M−H−182]$^-$, 663.0787, 481.0595, 300.9981		Slope	Unknown ellagitannin	$C_{42}H_{30}O_{27}$	966.0974	−0.93	
27	5.55	**1153.2655 [M−H]$^-$, 1027.2313, 1001.2095, 863.1843 [M−H−Cat−2]$^-$, 739.1646, 575.1180 [M−H−2(Cat−2)]$^-$, 413.0856, 287.0558**		277	Procyanidin tetramer	$C_{60}H_{50}O_{24}$	1154.2692	3.56	
28	5.61	**325.0900 [M−H]$^-$, 163.0403 [M−H−Hex]$^-$, 145.0298 [M−H−Hex−H_2O]$^-$, 187.0356**		312	Coumaric acid hexose (s)	$C_{15}H_{18}O_8$	326.1002	−7.07	Aaby et al. (2007), Määttä-Riihinen et al. (2004), Hukkanen et al. (2007) and Seeram et al. (2006)
29	5.62	**561.1400 [M−H]$^-$, 289.0741 [M−H−Afz]$^-$, 435.1101, 407.0797, 329.0699, 273.0745, 271.0602, 124.0251**		277	Propelargonidin dimer	$C_{30}H_{26}O_{11}$	562.1475	0.53	Gu et al. (2003)
30	5.69	967.0991 [M−H]$^-$, 665.0692 [M−H−HHDP]$^-$, 300.9984 [M−H−HHDP−364]$^-$		Slope	Unknown ellagitannin	$C_{42}H_{32}O_{27}$	968.1131	−6.41	
31	5.88	933.0627 [M−H]$^-$, 466.0245 [M−2H]$^{2-}$		Slope	Unknown ellagitannin				
32	5.90	**355.1050 [M−H]$^-$, 235.0604 [M−H−120]$^-$, 217.0512 [M−H−120−H_2O]$^-$, 193.0515 [M−H−Hex]$^-$, 175.0398 [M−H−Hex−H_2O]$^-$, 160.0157**		sh-328	Ferulic acid hexose	$C_{16}H_{20}O_9$	356.1107	5.91	
33	5.97	**849.2068 [M−H]$^-$, 577.1343 [M−H−Afz]$^-$, 289.0741 [M−H−Afz−Cat]$^-$, 723.1761, 559.1276, 451.1062, 397.0886, 287.0522, 289.0704, 125.0280**		278	Propelargonidin trimer	$C_{45}H_{38}O_{17}$	850.2109	4.36	Gu et al. (2003)
34	5.99	965.0895 [M−H]$^-$, 907.0804, 815.0911, 783.0660, 633.0701		Slope	Unknown ellagitannin	$C_{42}H_{30}O_{27}$	966.0974	−0.10	
35	6.15	**623.1247 [M−H]$^-$, 461.0700 [M−H−Hex]$^-$, 447.0890 [M−H−Gln]$^-$, 285.0390 [M−H−Hex−Gln]$^-$, 175.0251, 113.0233**	**625.1400 [M+H]$^+$, 449.1092 [M+H−Gln]$^+$, 287.0542 [M+H−Gln−Hex]$^+$**	264, 344	Kaempferol hexose glucuronide	$C_{27}H_{28}O_{17}$	624.1326	−0.16	
36	6.17	907.0888 [M−H]$^-$, 667.1490 [M−H−240]$^-$, 605.0740 [M−H−HHDP]$^-$, 300.9970 [M−H−HHDP−304]$^-$		n.a.	Unknown ellagitannin	$C_{40}H_{28}O_{25}$	908.0920	5.18	
37	6.20	**720.1570 [M−2H]$^{2-}$, 863.1812 [M−H−2Cat−2]$^-$, 575.1183 [M−H−2Cat−290]$^-$, 1151.2635, 965.2538, 693.1073, 577.1299, 449.082, 407.0736, 289.0717, 243.0298**		277	Procyanidin pentamer	$C_{75}H_{62}O_{30}$	1442.3326	−2.08	

(*continued on next page*)

Table 1 (*continued*)

Peak no.	R_t(min)	*m/z* ES(−)	*m/z* ES(+)	λ_{max} (nm)	Tentative structural assignment	Molecular formula	MM	Δmass (ppm)	Ref.
38	6.27	967.0996 [M−H]$^-$, 483.0447 [M−2H]$^{2-}$, 301.0003	969.1188 [M+H]$^+$, 303.0149	Slope	Unknown ellagitannin				
39	6.39	**577.1337 [M−H]$^-$, 289.0683 [M−H−Cat]$^-$, 451.1023, 425.0836, 407.0741, 245.0845, 125.0231**		n.a.	Procyanidin dimer or deriv, poss. acylated				
40	6.46	**355.1031 [M−H]$^-$, 193.0512 [M−H−Hex]$^-$, 295.0862, 235.0596, 175.0403, 160.0155**		sh-327	Ferulic acid hexose	$C_{16}H_{20}O_9$	356.1107	0.56	
41	6.47	981.0856 [M−H]$^-$, 481.0326		n.a.	Unknown ellagitannin	$C_{49}H_{26}O_{23}$	982.0865	7.03	
42	6.59	**463.0505 [M−H]$^-$, 300.9974**	465.0673 [M+H]$^+$, 303.0145 [M+H−Hex]$^+$	n.a.	Ellagic acid hexose	$C_{20}H_{16}O_{13}$	464.3392	−1.73	Hukkanen et al. (2007)
43	6.65	**635.0857 [M−H]$^-$, 465.0630 [M−H−Gallic acid]$^-$, 313.0540 [M−H−Gallic acid−Gall]$^-$, 169.0137**		272	Tris-galloyl-glucose	$C_{27}H_{24}O_{18}$	636.0963	−4.25	
44	7.01	933.0636 [M−H]$^-$, 466.0217[M−2H]$^{2-}$		Slope	Unknown ellagitannin	$C_{41}H_{26}O_{26}$	934.0712	0.21	
45	7.22	965.0902 [M−H]$^-$		Slope	Unknown ellagitannin	$C_{42}H_{30}O_{27}$	966.0974	0.62	
46	7.49	**785.0830 [M−H]$^-$, 615.0657 [M−H−Gall acid−2H$_2$O]$^-$, 300.9990, 463.0478**		270	Digalloyl-HHDP-glucose	$C_{34}H_{26}O_{22}$	786.0916	−0.89	
47	7.62	**639.1206 [M−H]$^-$, 337.0743, 301.0343, 178.9986**	**641.1380 [M+H]$^+$, 479.0841 [M+H−Hex]$^+$, 303.0508 [M+H−Hex−Gln]$^+$**	260, 353	Quercetin hexose glucuronide	$C_{27}H_{28}O_{18}$	640.1276	1.41	
48	7.81	**935.0781 [M−H]$^-$, 633.0720 [M−H−HHDP]$^-$, 300.9990, 467.0292 [M−2H]$^{2-}$**		Slope	Casuarictin	$C_{41}H_{28}O_{26}$	936.0869	−1.07	Hukkanen et al. (2007)
49	7.84	1235.0749 [M−H]$^-$, 617.0278 [M−2H]$^{2-}$		n.a.	Unknown ellagitannin	$C_{55}H_{32}O_{34}$	1236.0775	4.21	
50	8.04	933.0625 [M−H]$^-$, 466.0228 [M−2H]$^{2-}$		Slope	Unknown ellagitannin	$C_{41}H_{26}O_{26}$	934.0712	−0.96	
51	8.15	951.0709 [M−H]$^-$		n.a.	Unknown ellagitannin	$C_{41}H_{28}O_{27}$	952.0818	−3.26	
52	8.19	325.0918 [M−H]$^-$, 163.0412 [M−H−Hex]$^-$		n.a.	Coumaric acid hexose or deriv.[b]				
53	8.24	**934.0692 [M−2H]$^{2-}$, 1265.1743, 1235.0751, 783.0746, 633.0746, 469.0058, 300.9975**		Slope	Agrimoniin	$C_{82}H_{54}O_{52}$	1870.1581	−2.14	Hukkanen et al. (2007)
54	8.33	**935.0675 [M−H]$^-$, 633.0718 [M−H−HHDP]$^-$, 463.0447, 300.9978**		Slope	Potentillin	$C_{41}H_{28}O_{26}$	936.0869	−12.41	Hukkanen et al. (2007)
55	8.34	933.0647 [M−H]$^-$, 466.0231 [M−2H]$^{2-}$	935.0786 [M+H]$^+$, 917.0684 [M+H−H$_2$O]$^+$, 453.0097	Slope	Unknown ellagitannin	$C_{41}H_{26}O_{26}$	934.0712	1.39	
56	8.45	**433.0383 [M−H]$^-$, 300.9968 [M−H−Pent]$^-$**		253, 360	Ellagic acid pentose	$C_{19}H_{14}O_{12}$	434.0485	−5.54	Aaby et al. (2007), Määttä-Riihinen et al. (2004) and Hukkanen et al. (2007)
57	8.58	**609.1063 [M−H]$^-$, 301.0323**	**611.1220 [M+H]$^+$, 479.0811 [M+H−Pent]$^+$, 303.0514 [M+H−Pent−Gln]$^+$**	255, 353	Quercetin pentose glucuronide	$C_{26}H_{26}O_{17}$	610.1170	−4.76	
58	8.89	**639.1531 [M−H]$^-$, 459.0936, 314.0421, 299.0188, 271.0243, 255.0284, 243.0298**	**641.1705 [M+H]$^+$, 479.1162 [M+H−Hex]$^+$, 317.0653 [M+H−2Hex]$^+$, 302.0445, 285.0413**	253, 362	Isorhamnetin sophorose or di-hexose	$C_{28}H_{32}O_{17}$	640.1639	−4.69	
59	8.93	**623.1232 [M−H]$^-$, 337.0770, 285.0372, 113.0228**	625.1393 [M+H]$^+$, 647.122 [M+Na]$^+$, 463.0862 [M+H−Hex]$^+$, 287.0547 [M+H−Hex−Gln]$^+$	264, 346	Kaempferol hexose glucuronide	$C_{27}H_{28}O_{17}$	624.1326	−2.57	
60	8.95	447.0556 [M−H]$^-$, 300.9992	449.0723 [M+H]$^+$	252, 364	Ellagic acid deoxyhexose	$C_{20}H_{16}O_{12}$	448.0642	−1.79	Aaby et al. (2007) and Hukkanen et al. (2007)
61	9.01	**937.0935 [M−H]$^-$, 767.069 [M−H−Gall acid]$^-$, 300.997, 465.0754,** 468 0386 [M−2H]$^{2-}$		n.a.	Tris-galloyl-HHDP-glucose	$C_{41}H_{30}O_{26}$	938.1025	−1.28	n.a.
62	9.05	**300.9970 [M−H]$^-$, 283.9935, 257.006, 229.0137, 201.0191, 185.0236, 145.0293, 129.0334, 101.0369**	303.0139 [M+H]$^+$	253, 366	Ellagic acid	$C_{14}H_6O_8$	302.0063	−4.65	Aaby et al. (2007), Määttä-Riihinen et al. (2004), Hukkanen et al. (2007), Seeram et al. (2006) and Heur et al. (1992)

63	9.08	**493.0980 [M−H]$^-$, 341.0908, 281.0654, 251.0569, 221.0462, 179.0365**	495.1033 [M+H]$^+$, 325.0944 [M+H−Gall acid]$^+$, 163.0420 [M+H−Gall acid−Hex]$^+$	252, 367	Galloyl-caffeoyl-hexose	$C_{22}H_{22}O_{13}$	494.1060	−0.41	
64	9.12	**609.1508 [M−H]$^-$, 429.0805, 284.0327, 179.0035**	611.1622 [M+H]$^+$, 449.1063 [M+H−Hex]$^+$, 449.1063 [M+H−Hex]$^+$, 287.0559[M+H−2Hex]$^+$	n.a.	Kaempferol di-hexose	$C_{27}H_{30}O_{16}$	610.1534	8.54	
65	9.40	**593.1142 [M−H]$^-$ 307.0677, 285.0394, 113.0244**	**595.1340 [M+H]$^+$, 463.0828 [M+H−Pent]$^+$, 287.0550 [M+H−Pent−Gln]$^+$**	265, 345	Kaempferol pentose glucuronide	$C_{26}H_{26}O_{16}$	594.1221	−0.17	
66	9.40	965.0893 [M−H]$^-$, 783.0720		Slope	Unknown ellagitannin	$C_{42}H_{30}O_{27}$	966.0974	−0.31	
67	9.63	**787.0949 [M−H]$^-$, 617.0790 [M−H−Gall acid]$^-$, 465.0653 [M−H−Gall acid−Gall]$^-$, 635.0864, 169.0139,** 393 0429 [M−2H]$^{2-}$		278	Tetragalloylglucose	$C_{34}H_{28}O_{22}$	788.1072	−5.72	
68	9.83	933.0616 [M−H]$^-$, 466.0235 [M−2H]$^{2-}$, 301.0040		Slope	Unknown ellagitannin	$C_{41}H_{26}O_{26}$	934.0712	−1.93	
69	9.89	**623.1562 [M−H]$^-$, 459.1017, 314.0429, 299.0192, 271.0244, 255.0281, 243.0305, 227.0370, 199.0417**	**625.1781 [M+H]$^+$, 317.0666 [M+H−Rut]$^+$, 302.0436**	n.a.	Isorhamnetin rutinose or hexose-deoxyhexose	$C_{28}H_{32}O_{16}$	624.1690	−8.02	
70	9.96	**477.0675 [M−H]$^-$, 301.0363, 178.9986, 151.0034**	**479.0821 [M+H]$^+$, 303.0496 [M+H−Gln]$^+$, 113.0232**	255, 353	Quercetin glucuronide	$C_{21}H_{18}O_{13}$	478.0747	1.26	Aaby et al. (2007), Määttä-Riihinen et al. (2004), Hukkanen et al. (2007) and Seeram et al. (2006)
71	10.13	**725.1562 [M−H]$^-$, 681.1660, 501.0933, 314.0417, 299.0199, 271.0222, 243.0406, 227.0362**	**727.172 [M+H]$^+$, 565.1199 [M+H−Hex]$^+$, 317.0672 [M+H−Hex−Malhex]$^+$**	253, 360	Isorhamnetin hexose malonylhexose	$C_{31}H_{34}O_{20}$	726.1643	−0.41	
72	10.14	**463.0847 [M−H]$^-$, 300.0258, 301.0345, 271.0222**	465.1024 [M+H]$^+$, 303.0436 [M+H−Hex]$^+$	255, 353	Quercetin hexose	$C_{21}H_{20}O_{12}$	464.0955	−6.48	Aharoni et al. (2002), Määttä-Riihinen et al. (2004) and Seeram et al. (2006)
73	10.18	593.1140 [M−H]$^-$, 1187.2299 [2M−H]$^-$	**595.1268 [M+H]$^+$, 463.0867 [M+H−Pent]$^+$, 287.0554 [M+H−Pent−Gln]$^+$,** 1189.2547 [2M+H]$^+$	266, 345	Kaempferol pentose glucuronide	$C_{26}H_{26}O_{16}$	594.1221	−0.51	
74	10.94	**477.0990 [M−H]$^-$, 417.1188, 331.0720, 265.0698, 235.0641, 205.0507, 169.0140, 163.0340**	501.1019 [M+Na]$^+$, 309.0987 [M+H−Gall acid]$^+$, 147.0444 [M+H−Gall acid−Hex]$^+$	n.a.	Galloyl-coumaroyl hexose	$C_{22}H_{22}O_{12}$	478.1111	−9.01	
75	11.13	**549.0907 [M−H]$^-$, 505.1031, 463.3558, 300.0289**	551.1028 [M+H]$^+$, 303.0494 [M+H−Malhex]$^+$	n.a.	Quercetin malonylhexose	$C_{24}H_{22}O_{15}$	550.0959	4.92	Aaby et al. (2007)
76	11.39	1101.0745 [M−H]$^-$, 1083.0632 [M−H−H_2O]$^-$, 541.0205 [M−2H−H_2O]$^{2-}$, 949.0562 [M−H−H_2O−Gall]$^-$	1103.0871 [M+H]$^+$, 951.0761 [M+H−Gall]$^+$, 933.0671 [M+H−Gall−H_2O]$^+$	Slope	Unknown ellagitannin	$C_{48}H_{30}O_{31}$	1102.0771	4.72	
77	11.42	**939.1108 [M−H]− , 769.0878 [M−H−Gall acid]$^-$, 617.0743 [M−H−Gall acid−Gall]$^-$, 169.0127,** 469.0475 [M−2H]$^{2-}$		277	Pentagalloylglucose	$C_{41}H_{32}O_{26}$	940.1182	0.43	
78	11.50	1085.0710 [M−H]$^-$, 542.0278		Slope	Unknown ellagitannin				
79	11.67	**461.0729 [M−H]$^-$, 285.0411 [M−H−Gln]$^-$, 113.0243**	463.0868 [M+H]$^+$, 287.0557 [M+H−Gln]$^+$	263, 345	Kaempferol glucuronide	$C_{21}H_{18}O_{12}$	462.0798	1.95	
80	11.79	447.0898 [M−H]$^-$	449.1079 [M+H]$^+$, 287.0557 [M+H−Hex]$^+$	263, 345	Kaempferol hexose	$C_{21}H_{20}O_{11}$	448.1006	−6.49	Aaby et al. (2007)
81	11.96	933.0623 [M−H]$^-$, 466.0236 [M−H−H_2O]$^-$	935.0821 [M+H]$^+$, 303.0157	n.a.	Unknown ellagitannin	$C_{41}H_{26}O_{26}$	934.0712	−1.18	
82	12.41	1101.0701 [M−H]$^-$, 1083.0632 [M−H−H_2O]$^-$, 541.0205 [M−2H−H_2O]$^{2-}$, 949.0562 [M−H−H_2O−Gall]$^-$	1103.0871 [M+H]$^+$, 951.0761 [M+H−Gall]$^+$, 933.0671 [M+H−Gall−H_2O]$^+$	Slope	Unknown ellagitannin	$C_{48}H_{30}O_{31}$	1102.0771	0.73	
83	12.41	**491.0845 [M−H]$^-$, 315.0501 [M−H−Gln]$^-$, 300.0288, 255.0306, 271.0136, 151.0045, 113.0250**	**493.0992 [M+H]$^+$, 317.0713, 302.0443**	n.a.	Isorhamnetin glucuronide	$C_{22}H_{20}O_{13}$	492.0904	3.87	
84	12.66	1101.0716 [M−H]$^-$, 1083.0632 [M−H−H_2O]$^-$, 541.0205 [M−2H−H_2O]$^{2-}$, 949.0562 [M−H−H_2O−Gall]$^-$	1103.0871 [M+H]$^+$, 951.0761 [M+H−Gall]$^+$, 933.0671 [M+H−Gall−H_2O]$^+$	Slope	Unknown ellagitannin	$C_{48}H_{30}O_{31}$	1102.0771	2.09	

(*continued on next page*)

Table 1 (*continued*)

Peak no.	R_t(min)	*m/z* ES(−)	*m/z* ES(+)	λ_{max} (nm)	Tentative structural assignment	Molecular formula	MM	Δmass (ppm)	Ref.
85	13.09		535.1083 $[M+H]^+$, 287.0561 $[M+H-Malhex]^+$	n.a.	Kaempferol malonylhexose	$C_{24}H_{22}O_{14}$	534.1010	−0.93	Aaby et al. (2007) and Hukkanen et al. (2007)
86	14.42	1085.0763 $[M-H]^-$, 542.0291 $[M-2H]^{2-}$		Slope	Unknown ellagitannin	$C_{48}H_{30}O_{30}$	1086.0822	1.75	
87	14.48	967.0811 $[M-H]^-$, 949.0568 $[M-H-H_2O]^-$, 474.0230 $[M-2H-H_2O]^{2-}$, 931.0560 $[M-H-2H_2O]^-$, 465.0170 $[M-2H-2H_2O]^-$	969.0920 $[M+H]^+$, 951.0822 $[M+H-H_2O]^+$, 933.0628 $[M+H-2H_2O]^+$, 499.0719$[M+H-470]^+$, 337.0204 $[M+H-470-Hex]^+$	Slope	Unknown ellagitannin				
88	14.57	**417.2497 $[M-H]^-$, 463.2552 $[M-H+FA]^-$, 255.2130, 161.0502, 101.10249**	441.2477 $[M+Na]^+$, 419.2636 $[M+H]^+$, 401.2482 $[M+H-H_2O]^+$, 239.1982 $[M+H-H_2O-Hex]^+$, 383.2461 $[M+H-2H_2O]^+$, 221.1895 $[M+H-2H_2O-Hex]^+$, 203.1796 $[M+H-2H_2O-Hex-H_2O]^+$	n.d.	Sesquiterpenoid hexose	$C_{21}H_{38}O_8$	418.2567	2.16	
89	15.09	1101.0723 $[M-H]^-$, 1083.0632 $[M-H-H_2O]^-$, 541.0205 $[M-2H-H_2O]^{2-}$, 949.0562 $[M-H-H_2O-Gall]^-$	1103.0871 $[M+H]^+$, 951.0761 $[M+H-Gall]^+$, 933.0671 $[M+H-Gall-H_2O]^+$	Slope	Unknown ellagitannin	$C_{48}H_{30}O_{31}$	1102.0771	2.72	
90	15.55	**665.3888 $[M-H]^-$, 711.3932 $[M-H+FA]^-$, 503.3365 $[M-H-Hex]^-$, 207.0504**	667.4080 $[M+H]^+$, 689.3909 $[M+Na]^+$, 649.3980 $[M+H-H_2O]^+$, 631.3867 $[M+H-2H_2O]^+$, 487.3438 $[M+H-H_2O-Hex]^+$, 505.3535 $[M+H-Hex]^+$	n.d.	Triterpenoid hexose	$C_{36}H_{58}O_{11}$	666.3979	−1.95	
91	15.52	907.1207 $[M-H]^-$, 453.0510 $[M-2H]^{2-}$, 739.1131		Slope	Unknown ellagitannin	$C_{34}H_{36}O_{29}$	908.1342	−6.28	
92	15.90	**417.2473 $[M-H]^-$, 463.2502 $[M-H+FA]^-$, 255.1967 $[M-H-Hex]^-$, 161.0467, 113.0232, 101.0252**	441.2461 $[M+Na]^+$, 419.2636 $[M+H]^+$, 401.2482 $[M+H-H_2O]^+$, 239.1982 $[M+H-H_2O-Hex]^+$, 383.2461 $[M+H-2H_2O]^+$, 221.1895 $[M+H-2H_2O-Hex]^+$, 203.1796 $[M+H-2H_2O-Hex-H_2O]^+$	n.d.	Sesquiterpenoid hexose	$C_{21}H_{38}O_8$	418.2567	−3.59	
93	16.62	**665.3895 $[M-H]^-$, 711.3990 $[M-H+FA]^-$, 503.3365 $[M-H-Hex]^-$, 207.0518**	667.4080 $[M+H]^+$, 689.3909 $[M+Na]^+$, 649.3980 $[M+H-H_2O]^+$, 631.3867 $[M+H-2(H_2O)]^+$, 487.3438 $[M+H-H_2O-Hex]^+$, 505.3535 $[M+H-Hex]^+$	n.d.	Triterpenoid hexose	$C_{36}H_{58}O_{11}$	666.3979	−0.90	
94	16.63	**614.2483 $[M-H]^-$, 494.1889, 478.1976, 452.2183, 358.1383**	**616.2637 $[M+H]^+$, 454.2351 $[M+H-Caff]^+$, 470.2308 $[M+H-Coum]^+$, 308.1991 $[M+H-Caff-Coum]^+$, 163.0397 $[M+H-Caff-Coum-Sperm]^+$, 292.2010 $[M+H-Caff-Caff]^+$, 147.0453 $[M+H-Caff-Caff-Sperm]^+$, 220.0982**	218, 292	Di-caffeoyl coumaroyl spermidine	$C_{34}H_{37}N_3O_8$	615.2581	−3.09	
95	17.11	**417.2445 $[M-H]^-$, 463.2559 $[M-H+FA]^-$, 161.0408, 113.0223**	441.2461 $[M+Na]^+$, 419.2636 $[M+H]^+$, 401.2482 $[M+H-H_2O]^+$, 239.1982 $[M+H-H_2O-Hex]^+$, 383.2461 $[M+H-2H_2O]^+$, 221.1895 $[M+H-2H_2O-Hex]^+$, 203.1796 $[M+H-2H_2O-Hex-H_2O]^+$	n.d.	Sesquiterpenoid hexose	$C_{21}H_{38}O_8$	418.2567	−10.31	
96	17.22	**593.1253 $[M-H]^-$, 447.09 $[M-H-Coum]^-$, 285.04 $[M-H-Coum-Hex]^-$, 307.0806, 257.0396, 145.0293**	595.1431 $[M+H]^+$, 309.0981 $[M+H-Kaemp]^+$, 287.0560 $[M+H-Coum-Hex]^+$, 147.0444 $[M+H-Kaemp-Hex]^+$, 617.1258 $[M+H+Na]^+$	266, 314	Kaempferol coumaroyl hexose	$C_{30}H_{26}O_{13}$	594.1373	−7.08	Aaby et al. (2007), Seeram et al. (2006) and Tsukamoto et al. (2004)
97	17.71	**598.2556 $[M-H]^-$, 478.1959, 463.2223, 358.1390, 161.0244**	600.2705 $[M+H]^+$, 438.2392 $[M+H-Caff]^+$, 292.2023 $[M+H-Caff-Coum]^+$, 147.0448 $[M+H-Caff-Coum-Sperm]^+$, 454.2359, 420.2293, 204.1012	218, 292	Caffeoyl di-coumaroyl spermidine	$C_{34}H_{37}N_3O_7$	599.2632	0.50	
98	18.04	**593.1299 $[M-H]^-$, 447.0900 $[M-H-Coum]^-$, 285.0400 $[M-H-Coum-Hex]^-$, 307.0820, 255.0304, 145.0315**	**595.1431 $[M+H]^+$, 309.0981 $[M+H-Kaemp]^+$, 287.0560 $[M+H-Coum-Hex]^+$, 147.0444 $[M+H-Kaemp-Hex]^+$,617 1258 $[M+H+Na]^+$**	n.a.	Kaempferol coumaroyl hexose	$C_{30}H_{26}O_{13}$	594.1373	0.67	Aaby et al. (2007), Seeram et al. (2006) and Tsukamoto et al. (2004)
99	18.07	**598.2514 $[M-H]^-$, 478.1942, 436.2213, 358.1374, 316.1657, 161.0234**	**600.2665 $[M+H]^+$, 438.2383 $[M+H-Caff]^+$, 454.2310 $[M+H-Coum]^+$, 292.2008 $[M+H-Caff-Coum]^+$, 147.0400 $[M+H-Caff-Coum-Sperm]^+$, 163.0392, 204.1013, 318.1806**	218, 292	Caffeoyl di−coumaroyl spermidine	$C_{34}H_{37}N_3O_7$	599.2632	−6.52	
100	18.50	**628.2635 $[M-H]^-$, 508.2013, 478.1971, 358.1451**	**630.2792 $[M+H]^+$, 454.2346 $[M+H-Fer]^+$, 468.2503 $[M+H-Caff]^+$, 484.2456 $[M+H-Coum]^+$, 177.0555 $[M+H-Coum-Caff-Sperm]^+$, 163.0387, 204.100, 234.1153, 450.2380**	225, 301	Caffeoyl coumaroyl feruoyl spermidine	$C_{35}H_{39}N_3O_8$	629.2737	−3.82	
101	19.05	**471.1288 $[M-H]^-$, 427.1464, 325.0983, 307.0796, 247.0640, 163.0397, 145.0303, 119.0501**	495.1288 $[M+Na]^+$, 309.0998 $[M+H-H_2O-Coum]^+$, 291.0887 $[M+H-H_2O-Coum-H_2O]^+$, 147.0451 $[M+H-H_2O-Coum-Hex]^+$	n.a.	Di-coumaroyl hexose	$C_{24}H_{24}O_{10}$	472.1369	−0.64	
102	19.35	582.255 $[M-H]^-$	**584.275 $[M+H]^+$, 438.2391 $[M+H-Coum]^+$, 292.2036 $[M+H-Coum-Coum]^+$, 147.0449 $[M+H-Coum-Coum-Sperm]+$, 420.2306, 275.1763, 204.1017, 217.1354, 318.1834**	290	Tri coumaroyl spermidine	$C_{34}H_{37}N_3O_6$	583.2682	−9.27	

103	19.78	**612.2673 [M−H]$^-$, 492.2097, 372.1502**	**614.2854 [M+H]$^+$, 468.2500 [M+H−Coum]$^+$, 438.24 [M+H−Fer]$^+$, 147.0447 [M+H−Fer−Coum−Sperm]$^+$, 177.0544, 204.1035, 275.1763, 292.2064, 420.2299**	292	Feruoyl dicoumaroyl spermidine	$C_{35}H_{39}N_3O_7$	613.2788	−6.04
104	20.15	**642.2834 [M−H]$^-$, 522.2189, 492.2143, 372.1505, 175.0389, 149.0559, 119.0493**	**644.2970 [M+H]$^+$, 468.2500 [M+H−Fer]$^+$, 322.2200 [M+H−Fer−Coum]$^+$, 177.053 [M+H−Fer−Coum−Sperm]$^+$, 498.2608, 450.2401, 305.1911, 318.1787, 234.1038**	293	Coumaroyl diferuoyl spremidine	$C_{36}H_{41}N_3O_8$	643.2894	2.96
105	20.67	**649.3942 [M−H]$^-$, 695.4033 [M−H+FA]$^-$, 487.3413 [M−H−Hex]$^-$, 207.0410,** 1299.7960 [2M−H]$^-$, 1137.7527 [2M−H−Hex]$^-$		n.d.	Triterpenoid hexose	$C_{36}H_{58}O_{10}$	650.4030	−1.54
106	20.97	**649.4076 [M−H]$^-$, 695.3997 [M−H+FA]$^-$, 487.3395 [M−H−Hex]$^-$, 207.0512,** 1299.7960 [2M−H]$^-$, 1137.7527 [2M−H−Hex]$^-$		n.d.	Triterpenoid hexose	$C_{36}H_{58}O_{10}$	650.4030	19.09
107	21.63	**649.3986 [M−H]$^-$, 487.3447 [M−H−Hex]$^-$, 695.3958 [M−H+FA]$^-$, 207.0483,** 1299.7966 [2M−H]$^-$, 1137.7478 [2M−H−Hex]$^-$	673.3925 [M+Na]$^+$, 407.3311	n.d.	Triterpenoid hexose	$C_{36}H_{58}O_{10}$	650.4030	5.24
108	22.18	**649.3927 [M−H]$^-$, 695.3995 [M−H+FA]$^-$, 487.3447 [M−H−Hex]$^-$, 207.0475,** 1299.7877 [2M−H]$^-$, 1137.7477 [2M−H−Hex]$^-$	673.3942 [M+Na]$^+$, 489.3573 [M+H−Hex]$^+$, 407.3317	n.d.	Triterpenoid hexose	$C_{36}H_{58}O_{10}$	650.4030	−3.85
109	23.40	**649.3954 [M−H]$^-$, 695.3997 [M−H+FA]$^-$, 487.343 [M−H−Hex]$^-$, 207.0576,** 1299.8065 [2M−H]$^-$, 1137.7521 [2M−H−Hex]$^-$ 1153.7471, 503.3373	673.3938 [M+Na]$^+$, 489.3578 [M+H−Hex]$^+$, 407.3305	n.d.	Triterpenoid hexose	$C_{36}H_{58}O_{10}$	650.4030	0.31

The reported fragments were observed in source and verified through MS/MS analysis of the parental ion (MS/MS fragments marked bold). λ_{max} is the absorbance maxima in the UV/visible range, when marked as 'slope' refers to typical ellagitannin UV/visible spectrum as shown in Fig 6B. n.a., not available; n.d., not detected. MM, molecular monoisotopic mass of the putative metabolite. Δppm, deviation of the observed ion mass from the corresponding calculated monoisotopic mass. (s) indicates identification based on standard compound. Ref., previous reports on metabolites in strawberry.

[a] Catechin was identified (distinguished from epi-catechin) based on the elution order in our parallel study on strawberry fruit (Fait et al., 2008).

[b] The correct molecular ion was not determined and thus mol. formula is not available.

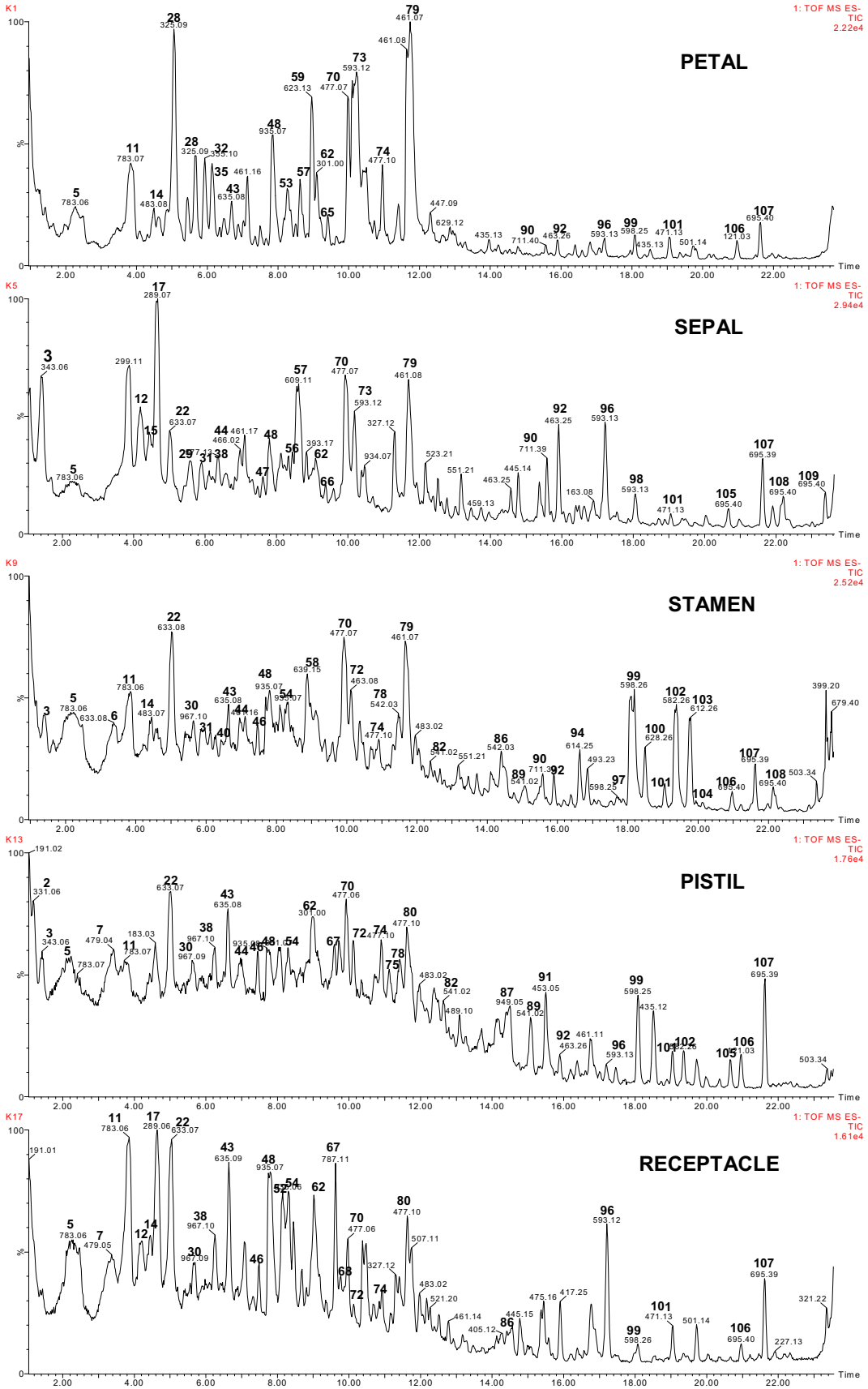

Fig. 2. UPLC-qTOF-MS total ion current chromatograms in ES(−) of strawberry floral organs. The peaks are marked by numbering that refers to tentative identity in Table 1.

caffeic and ferulic acids in a total of seven chromatographic peaks (**94, 97, 99, 100, 102, 103, 104**). The use of the Elemental composition calculator (as a part of the MassLynx software) allowed the correct elemental composition prediction for all the nitrogen

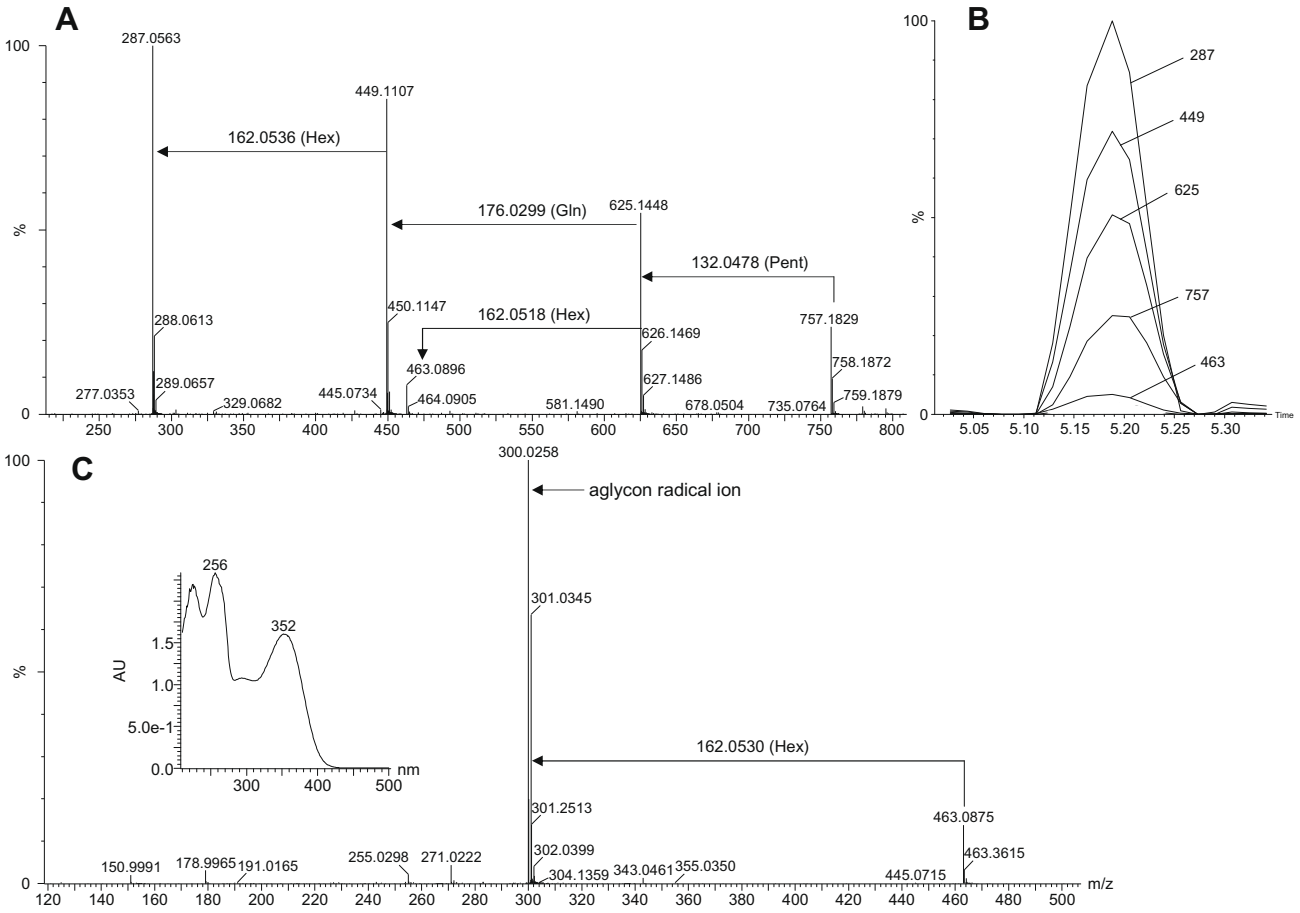

Fig. 3. Flavonol fragmentation in 20 eV ESI. (A) In source fragmentation of kaempferol pentose-hexose-glucuronide (**20**) in ES(+); (B) reconstructed ion chromatograms of each of the fragments resulting from the compound in A; (C) MS/MS fragmentation of quercetin hexose (**72**) in ES (−). The UV/visible spectrum of the compound is embedded. An additional ion is observed due to flavonol aglycon radical formation (marked in the figure). Hex, hexose; Gln, glucuronide; Pent, pentose.

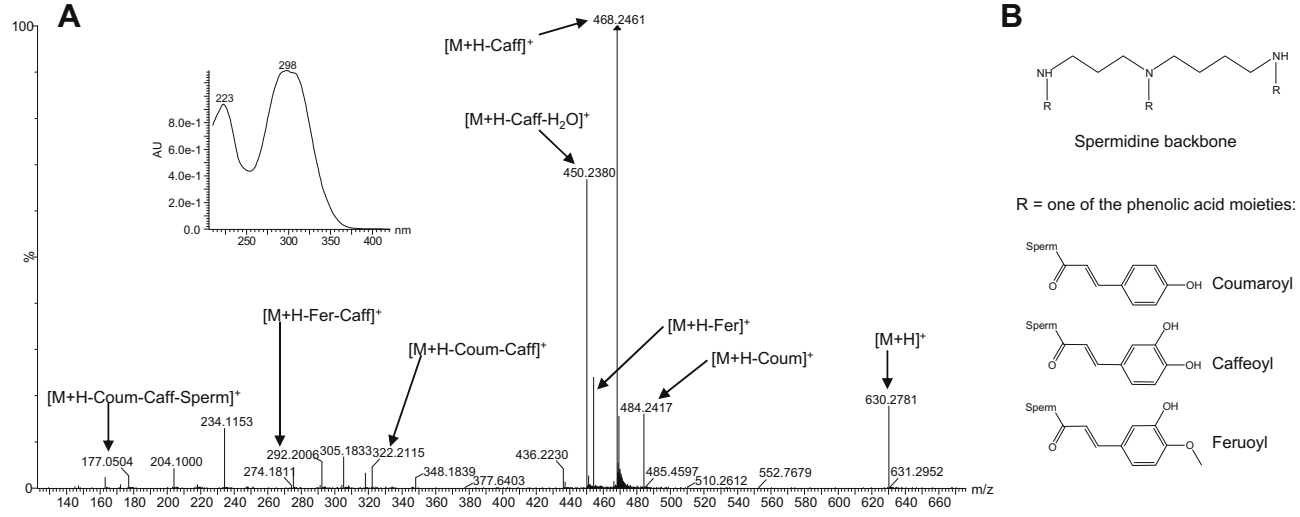

Fig. 4. Spermidine derivative detected in stamen of strawberry flower. (A) MS/MS spectrum of caffeoyl coumaroyl feruoyl spermidine (**100**) in ES(+). The UV/visible spectrum of the compound is embedded; (B) chemical structures of the spermidine molecule and the phenolic acid moieties observed in the compound in A.

containing compounds reported here while the accurate mass spectral information enabled the identification of losses of acyl moieties and distinguishing them from sugar moieties possessing only slight difference in their molecular weight (Tables 1 and 2). The characteristic MS/MS fragmentation is exemplified by the analysis of caffeoyl coumaroyl feruoyl spermidine (**100**), in which the signal of *m/z* 177.0504 amu corresponds to the feruoyl moiety retaining the charge (Fig. 4A). Identity of the compounds was verified by characteristic UV spectra showing λ_{max} at 290–300 nm and the matching of the suggested molecular formula to the corresponding compounds presented in the Dictionary of Natural Products (DNP) and SciFinder. The chemical structure of the spermidine

Table 2
Neutral losses and adduct ions monitored in the study

Adducts	
Ion name	Ion mass
ES(+)	
M+H	M+1.0078
M+Na	M+22.9898
M+K	M+38.9637
2M+H	2M+1.0078
ES(−)	
M−H	M−1.0078
M+FA−H	M+44.9977
2M−H	2M−1.0078
Neutral losses, ES(+) and ES(−)	
Moiety	Monoisotopic mass
H_2O	18.0106
Pentose	132.0423
Deoxyhexose	146.0579
Hexose	162.0528
Glucuronide	176.0321
Rutinose	308.1107
Caffeoyl	162.0317
Coumaroyl	146.0368
Sinapoyl	206.0579
Feruoyl	176.0473
Galloyl	152.011
Acetyl	42.0106
Malonyl	86.0004
Acetylhexose	204.0423
Malonylhexose	248.0532
Coumaroylhexose	308.0896
Methylhexose	176.0675

backbone and the phenolic acid moieties observed are shown in Fig. 4B. However, the exact position of each moiety was not determined in the backbone, although the substitution is known to occur on the nitrogen atoms of the spermidine backbone (Werner et al., 1995).

In the last few minutes of the chromatographic run, particularly in the sepal extracts, we observed a series of mass peaks that did not exhibit clear UV absorbance. The peaks **105–109** exhibit the putative elemental composition of $C_{36}H_{58}O_{10}$, which generates 36 hits in the DNP (2 antibiotics, 3 xylopyranoside derivatives of terpenoids and 31 triterpenoid glucopyranosides). All the five peaks had the proposed deprotonated molecular ions of *m/z* 649.39 and an aglycon fragment of *m/z* 487.34, showing the loss of hexose sugar and aglycon matching with oleanenoic or ursenoic acid-type triterpenoids (Table 1, Fig. 5A). A compound called tormentic acid retains an aglycon of the same size and has been reported several times in the *Rosaceae* family, e.g., in *Rubus rosaefolius* (Kanegusuku et al., 2007) and *Rubus cochinchinensis* (Lien et al., 1999). For two peaks (**90** and **93**), we obtained a putative formula of $C_{36}H_{58}O_{11}$ that had 41 hits in the DNP search (40 triterpenoid glucopyranosides and 1 other terpenoid derivative). The two compounds have similar hexose sugar fragmentation and the deprotonated aglycon of *m/z* 503.34 that also suggests an oleanenoic or ursenoic acid backbone (Table 1, Fig. 5B). The molecular weights and formulae of these two compounds are similar to the one of the triterpenoid Niga-ichigoside F1 found in the genus *Rubus* of the family *Rosaceae* (Nam et al., 2006; Ardenghi et al., 2006). The molecules described above represent relatively complex structures with several methyl moieties in the backbone. These features could result in a late elution in the chromatographic run performed in this study. In addition, the LogD (pH 3) value for these compounds is fairly high (3,8, SciFinder) that is typical for hydrophobic compounds and further explains the late elution time. Furthermore, the lack of chromophores in the molecular structure could explain the absence of UV spectra. All these putative triterpenoids showed adduct formation (formate in negative mode and sodium in positive mode), and such behavior has been reported earlier in LC–MS analysis of triterpenoids (Huhman and Sumner, 2002; Madl et al., 2006). The above results let us suggest that the compounds occurring in peaks **90**, **93** and **105–109** are triterpenoid glucopyranoside derivatives (saponins), that occur in different (stereo)isoforms.

Three peaks (**88**, **92** and **95**), eluting in the same area in the chromatogram as the predicted triterpenoids, exhibited the same adduct ions and also lacked absorbance in UV. These compounds were smaller in size compared to the triterpenoid derivatives (quasi-molecular ion *m/z* 417.25 in negative ESI) and showed a loss of one hexose (Table 2, Fig. 5C). The suggested molecular formula of $C_{21}H_{38}O_8$ and a search in the DNP generated hits to sesquiterpenoid compounds such as eudesmanetriol (8 hits) or farnesadiene (4 derivatives). Taking into account the structural relationship to the triterpenoids, these peaks were tentatively assigned as hexose derivatives of sesquiterpenoid compounds, which are often detected in conjunction with triterpenoids (Laphookhieo et al., 2004; Shen et al., 2007).

2.4. Major differences exist in between the metabolite profiles of strawberry flower organs

The data collected from the UPLC-qTOF-MS analysis was used to determine the proportional amounts of individual compounds in different organs based on the base peak area of each molecular ion spectrum whenever possible. As no standards were used and the ionization efficiencies or ion suppression were not measured, we only compared the levels of individual metabolites across the different floral organs and not between different metabolites. The occurrence of each metabolite in the different organs is presented in a heat map (Fig. 7). The base peak response area values for each of the metabolites are included as Supplementary material (Table S1). The majority of the peaks that were tentatively assigned represented ellagitannins while the second largest metabolite class were the flavonols. All the metabolite classes exhibited different patterns of accumulation between the five flower organs.

2.5. Strawberry flower petals are rich in flavonols and phenolic acids

Extracts of strawberry flower petals contained mainly phenolic acids and flavonols (Fig. 7). Phenolic acids are hydroxylated derivatives of benzoic and cinnamic acids and are frequently conjugated with sugars. They serve as precursors for a wide array of secondary metabolites including: benzoates, salicylates, coumarins, lignans, lignin and flavonoids. Among the detected phenolic acid derivatives present in the petals was coumaric acid-hexose. Coumaroyl-CoA, derived from a coumarate precursor, is the substrate for chalcone synthase which initiates the flavonoid biosynthetic pathway. Among the floral flavonoids, the petals had the largest proportion of kaempferol derivatives, which gives a logical explanation for the presence of the precursor phenolic acid. The compounds that contribute to the flavor and aroma of ripe strawberry fruit and several enzymes involved in their biosynthesis have been characterized earlier (Aharoni et al., 2000; Lunkenbein et al., 2006). Many of these compounds are methylated volatile derivatives of phenolic acid precursors, synthesized in a branch of the phenylpropanoid pathway (Zabetakis and Holden, 1997). It may be that strawberry petals also require phenolic acids as precursors for generating scent components. However, volatile compounds were not analyzed in this study and the composition of strawberry flower volatiles were not yet described.

While ellagitannins were present in all floral organs, the lowest proportion was found in petals. The majority of ellagitannins detected in petals has been previously identified in strawberry fruit

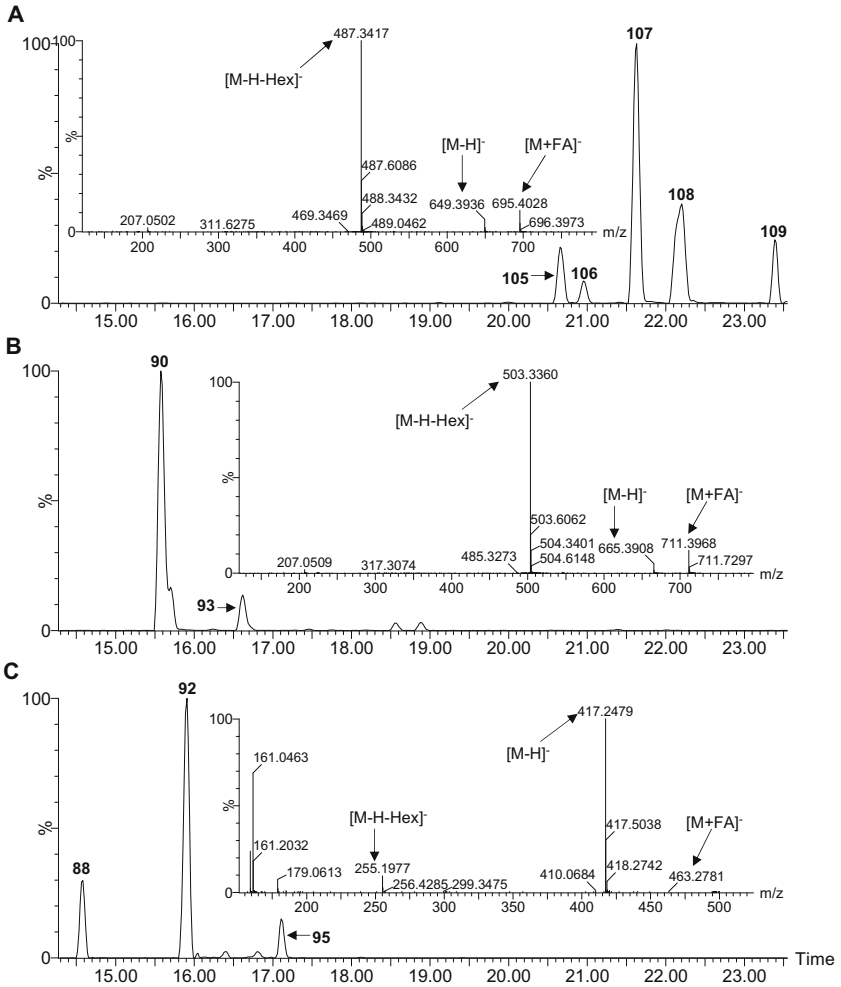

Fig. 5. Reconstructed ion chromatograms and MS/MS fragmentation in ES(−) of tentative terpenoid derivatives in strawberry sepals. (A) Triterpenoid saponin MW 650, inserted MS/MS spectrum of the ion *m/z* 695, (B) triterpenoid saponin MW 666, inserted MS/MS spectrum of the ion *m/z* 711 and (C) sesquiterpenoid hexose of MW 418, inserted MS/MS spectrum of the ion *m/z* 463. The peak numbers refer to the names listed in Table 2. $[M+FA]^-$ indicates a formic acid adduct of the molecular ion.

A

Metabolite	*m/z* $[M-H]^-$	Formula
1. Galloyl-glucose	331.06	$C_{13}H_{16}O_{10}$
2. Di-galloyl-glucose	483.08	$C_{20}H_{20}O_{14}$
3. Tris-galloyl-glucose	635.09	$C_{27}H_{24}O_{18}$
4. Tetra-galloyl-glucose	787.09	$C_{34}H_{28}O_{22}$
5. Penta-galloyl-glucose	939.11	$C_{41}H_{32}O_{26}$
6. HHDP-glucose	481.06	$C_{20}H_{18}O_{14}$
7. Galloyl-HHDP-glucose	633.07	$C_{27}H_{22}O_{18}$
8. Di-galloyl-HHDP-glucose	785.08	$C_{34}H_{26}O_{22}$
9. Tri-galloyl-HHDP-glucose	937.09	$C_{41}H_{30}O_{26}$
10. Bis-HHDP-glucose	783.06	$C_{34}H_{24}O_{22}$
11. Bis-HHDP-galloyl-glucose	935.07	$C_{41}H_{28}O_{26}$

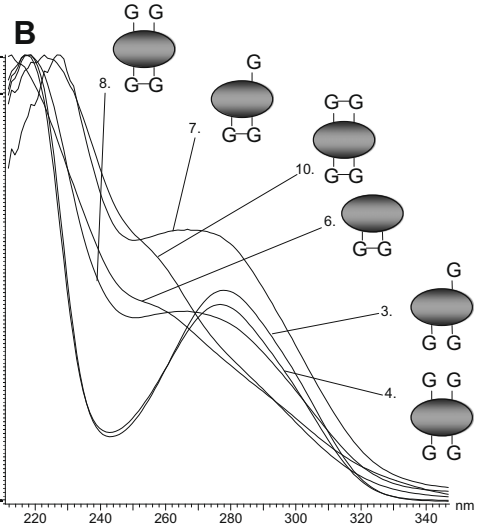

Fig. 6. Typical ellagitannin features in LC-PDA-MS analysis. (A) Diagnostic molecules/fragments used in the identification of ellagitannin peaks and (B) UV spectrum of only galloyl-moieties (tris-galloyl-glucose, tetra-galloyl-glucose), only HHDP (HHDP-glucose, bis-HHDP-glucose) and both galloyl and HHDP (galloyl-HHDP-glucose, di-galloyl-glucose) containing molecules. The schematic presentation is a simplified model of the ellagitannin backbones, in which gray oval represents the sugar core and 'G' stands for galloyl, the connection of the two represents the HHDP unit.

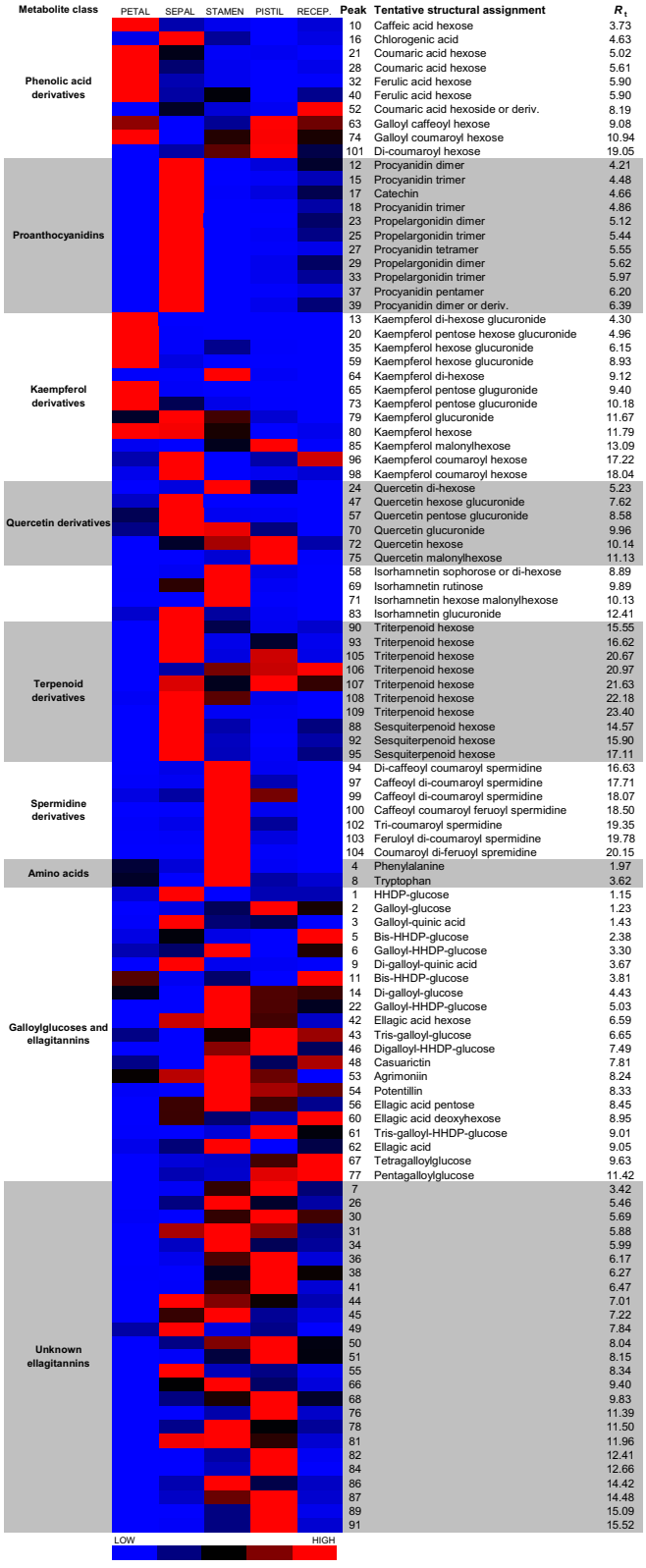

Fig. 7. Occurrence of tentatively identified metabolites in strawberry flower organs. The colours indicate the proportional distribution of each putatively identified metabolite among the flower organs as determined by the average peak response area. The analysis was done in a Microsoft Excel – implemented macro program available at http://www.senorjosh.com/archives/2003/04/heatmap_tool_vba.shtml. The metabolite numbers refer to the Table 1, exact peak response area values for each metabolite are provided in Table S1.

and leaves, namely agrimoniin (**53**), casuarictin (**48**), bis-HHDP-glucose (**5, 11**) and galloyl-HHDP-glucose (**6, 22**); as well as the ellagitannin precursors di-galloyl-glucose (**14**) and tris-galloyl glucose (**43**) (Okuda et al., 1992; Mullen et al., 2003; Hukkanen et al., 2007). The two aromatic amino acids phenylalanine and tryptophan, as well as traces of terpenoids were also detected in the petals. On the other hand, spermidines and proanthocyanidins were absent from petals apart from caffeoyl di-coumaroyl spermidine, which was detected as low signal (Fig. 7, Table S1).

2.6. Sepals contain the majority of floral proanthocyanidins and terpenoid saponins

Strawberry sepals contained compounds belonging to all the different metabolite classes identified in this study (Fig. 7). Only spermidine derivatives were nearly absent, as trace signals of caffeoyl-di-coumaroyl-, tris-coumaroyl-, and di-caffeoyl-coumaroyl spermidine were detected (Table S1). The major classes of compounds that accumulated in the sepals were proanthocyanidins and terpenoids. In fact, the presence of proanthocyanidins was restricted to the sepal and receptacle, while only trace signals were observed in the stamen, pistil and petals (Fig. 7). Proanthocyanidins (condensed tannins) occur widely as end products of the flavonoid pathway and plants produce them for the protection against predation (Poter, 1994; Dixon et al., 2005). Proanthocyanidins are highly antioxidative molecules that also contribute to the health-beneficial effect of flavonoid-rich diet (Santos-Buelga and Scalbert, 2000). All the proanthocyanidins detected in this study were oligomers of procyanidin and propelargonidin, in accordance with an earlier study on strawberry fruit (Gu et al., 2003). As the main role of the sepals is to shield the floral bud against environmental stress factors like fungal diseases, the presence of these defense molecules might be part of the general bud protection mechanism. The presence of proanthocyanidins in sepals was not described earlier, although they are commonly observed in other green tissues of plants, including strawberry leaves (Hukkanen et al., 2007).

Triterpenoid saponins (glycosylated triterpenoids) are a structurally diverse class of natural products whose biological role in plants is not clearly defined. They are suggested to serve as antimicrobials and antifeedants (Osbourn, 2003; Sparg et al., 2004). Unlike flavonoids, terpenoids do not absorb UV/visible light or exhibit radical scavenging activity (Spitaler et al., 2006). Mono- and sesquiterpenes are also essential part of floral scent mixtures of various species (Pichersky et al., 1994; Aharoni et al., 2005). Triterpenoids have been reported to accumulate in the floral tissues of *Calendula officinalis* (Ukiya et al., 2006), and another group of terpenoid derivatives, sesquiterpenoids, have been detected in *Arnica montana* flowers (Spitaler et al., 2006). In this study, seven triterpenoid saponins along with three sesquiterpenoid derivatives were tentatively assigned, most of them with highest occurrence in sepals (Fig. 7). The antifeedant characteristic of terpenoids complements the defence role of the compounds in the flavonoid pathway, and is in line with the need for an efficient protection against pathogens, particularly at the early stages of flower development. The presence of these defensive metabolites at a late stage of flower development (as detected in this study), suggests that the protective role of proanthocyanidins and terpenoids is important also after the flower bud phase. Several terpenoid compounds similar in structure to those reported here have been detected also in other species of the *Rosaceae* family (Guo et al., 1998; Meesapyodsuk et al., 2007; Nam et al., 2006; Ardenghi et al., 2006; Kanegusuku et al., 2007).

2.7. The majority of secondary metabolites in strawberry pistil are ellagitannins

Crop species of the *Rosaceae* family are known as important dietary sources of ellagic acid and ellagitannins (Koponen et al., 2007).

Ellagitannins have gained large attention during the past years, as they have been shown to exhibit important bioactive characteristics, being antioxidative (Mertens-Talcott et al., 2006; Yu et al., 2005) and anticarcinogenic (Kuo et al., 2007; Ross et al., 2007; Seeram et al., 2006). The pistil of strawberry flower contained the highest proportion of ellagitannins (hydrolysable tannins) compared to the other strawberry flower organs. In addition to the pistil, the levels of ellagitannins were relatively high in stamen and receptacle, but quantitative differences were observed in different ellagitannins derivatives among the organs (Fig. 7). For example, HHDP-glucose (**1**), galloylquinic acid (**3**), digalloylquinic acid (**9**) accumulated in the sepals and bis-HHDP-glucose (**11**), tetragalloylglucose (**67**), pentagalloylglucose (**77**) in the receptacle. Among the ellagitannins that could not be precisely annotated (Fig. 7; "Unknown ellagitannins"), the quasi-molecular ions of *m/z* 967.10 (putative uncharged molecule; $C_{42}H_{32}O_{27}$) in three peaks (**30**, **38**, **87**) and *m/z* 1101.07 (putative uncharged molecule, $C_{48}H_{30}O_{31}$) in four peaks (**76, 82, 84, 89**) were predominantly present in the pistil. The actual role of the various ellagitannin derivatives in flower organs is of interest and it might be related to mechanisms of defense as in the case of other flower metabolites such as the proanthocyadins and triterpenoids.

All the other metabolite classes identified in this study were also present in the pistil, including two phenolic acid derivatives (galloyl-caffeoyl-hexose, **63**; and di-coumaroyl hexose, **101**) that were most abundant in pistil (Fig. 7). Also the most abundant triterpenoid observed among all the flower organs displayed the highest levels in the pistil (**107**).

2.8. A variety of hydroxycinnamic acid substituted spermidines accumulate in the stamen

Polyamines are nitrogenous compounds which might be conjugated with small molecules such as phenolic acids. These conjugates have been particularly studied in flowers (Martin-Tanguy, 1997), and were characterized from strawberry and flowers of other *Rosaceae* species (Sood and Nagar, 2004; Starck et al., 1990). All the seven spermidine derivatives detected in this study were most abundant in stamen, while much lower levels were detected in other flower organs (Fig. 7). This is in accordance with a previous study in which spermidines were detected in the stamen of various species in the genus *Aphelandra* (Werner et al., 1995). Diamine-putrescine, triamine-spermidine and tetramine-spermine are growth regulators that participate in a variety of processes in plants including growth, embryogenesis, flowering and senescence (Kumar et al., 1997; Facchini et al., 2002). Acyl-conjucated spermidines have been studied in Rosaceae flowers (Starck et al., 1990) and are also known to participate in the floral induction of strawberry (Tarenghi and Martin-Tanguy, 1995). The presence of polyamines is essential for flower development (Kumar et al., 1997), but their precise function is not defined. In this study the filaments and anthers were not dissected, but in earlier studies polyamines have been detected particularly in the anthers and were suggested to participate in pollen formation (Werner et al., 1995).

As in the case of the pistil, ellagitannins were also abundant in the stamen (Fig. 7). Several ellagitannins previously characterized in other strawberry tissues (fruit and leaves) accumulated to the highest levels in the stamen, including galloyl-HHDP-glucose (**6, 22**), casuarictin (**48**), agrimoniin (**53**) and potentillin (**54**) (Hukkanen et al., 2007; Aaby et al., 2007). In addition, several compounds classified as ellagitannins (Fig. 7, "Unknown ellagitannins") were most abundant in the stamen. Among those were compounds detected in four peaks with the deprotonated *m/z* of 965.09 (uncharged molecule; $C_{42}H_{30}O_{27}$, single hit in the DNP for Rhoipteleanin H, peaks **26**, **34**, **45**, **66**). The compound represented by *m/z* 965.09 is 2 amu smaller than the *m/z* 967.10 ellagitannin compound detected in the pistil (see above). This 2 amu difference in the size of ellagitannins may result from an additional interlinkage between adjacent galloyl moieties by oxidation, which is typically observed in ellagitannin biosynthesis (Niemetz and Gross, 2005). Since these two compounds were detected in separate flower organs, a specific enzyme responsible for this additional modification might be present in the stamen but not in the pistil.

2.9. The metabolite profile of the receptacle resembles the one of early strawberry fruit development

Ellagitannins were also the main metabolite class detected in the receptacle extracts (Fig. 7). The early developing strawberry fruit (swollen, mature receptacle) contains an array of ellagitannins similar to the ones detected in the receptacle studied here. Two bis-HHDP-glucoses (**5**, **11**) were particularly abundant in the receptacle and are also present in the mature strawberry fruit (Aaby et al., 2007). Various substituted galloylglucoses (from monogalloylglucose to pentagalloylglucose) that serve as precursors for ellagitannin biosynthesis were detected in the receptacle. Tetra- (**67**) and pentagalloylglucose (**77**) were the predominant derivatives, which indicate that ellagitannin biosynthesis starts already at a very early stage of strawberry fruit maturation (Fig. 7). However, the differences in the abundance of the observed signals between the compounds belonging to the same metabolite class (i.e. bis-HHDP-glucoses and galloylglucoses) may also be due to differential ionization effects. The exact concentrations of each of the metabolite would require application of standard compounds in known concentrations. Galloylglucose (**2**) has been reported to be present at the early stages of fruit maturation (Aharoni et al., 2002). Several uncharacterized ellagitannins (Fig. 7; "Unknown ellagitannins") were also detected in the receptacle, but they did not accumulate to the same level as detected in the stamen or pistil, and none of them were predominantly or exclusively present in the receptacle. The amount of free ellagic acid (**62**) and two of its sugar conjugates (deoxyhexose, **60**; and pentose, **56** derivatives) were relatively high in the receptacle, as in the case of the early stages of strawberry maturation (Aharoni et al., 2002). Only trace amounts of cinnamic acid derivatives (coumaric **21**, **28**; caffeic, **10;** and ferulic **32**, **40** acid hexoses) were detected in the receptacle, in accordance with previous results which indicated that phenolic acids accumulate mainly in the mature strawberry fruit (Aharoni et al., 2002; Halbwirth et al., 2006).

The receptacle also contained high amounts of proanthocyanidins, mainly catechin (**17**) and the procyanidin dimer (**12**). Early developing strawberry fruit exhibit high content of large proanthocyanidin polymers (Halbwirth et al., 2006; Fait et al., 2008), and the presence of smaller oligomers in the receptacle indicates that the synthesis of proanthocyanidins starts already at the flower stage.

2.10. Strawberry floral organs display particular profiles of flavonols

All flavonoids detected in this study were derivatives of the flavonols kaempferol and quercetin (Table 1). Flavonols play several roles in higher plants including the contribution to abiotic and biotic stress tolerance (Groteweld, 2006) and in fertility, being essential for pollen tube germination (Mo et al., 1992; Ylstra et al., 1994). Another essential role for flavonols in the flower is to act as co-pigments alongside the anthocyanins (Nielsen et al., 2005; Fukui et al., 2003). However, in strawberry flowers this role is not apparent since no anthocyanins were detected in the floral tissues in the present study. This might also explain why no flavones were detected in the present study, as flavones are reported to be stronger co-pigments than the flavonols (Fukui et al., 2003).

Altogether 13 peaks were tentatively assigned as kaempferol derivatives (Table 1). The majority of kaempferol derivatives were detected at highest in the petal or sepal tissues (Fig. 7). The most abundant substituents were glucuronide (**79**), pentose-glucuronide (**73**) and hexose-glucuronide (**59**), which were present in all flower organs at varying amounts (Fig. 7). Kaempferol coumaroyl hexose (**96**, **98**) had a distinct distribution pattern, as both isomers were most abundant in the sepal and receptacle tissues (Fig. 7). The pentose-glucuronide conjugates of flavonols might be specific for *Rosaceae*, as there are only a few studies reporting them, all in *Rosaceae* family members (Rommel and Wrolstad, 1993).

Quercetin was found as an aglycone in six peaks, whereas the methylated form of quercetin, i.e. isorhamnetin, was detected in four different peaks in the chromatogram (Fig. 7). The profiles of these two flavonols among the floral organs were different from the one observed for kaempferol (Fig. 7). Quercetin was detected mostly in the sepals and stamens, while as mentioned above kaempferol was detected in sepals and petals. The most intensive signal came from quercetin glucuronide (**50**) which showed a similar profile to the one of kaempferol glucuronide, being highest in the sepal and stamen, but also present in the petal, pistil and receptacle tissues (Fig. 7). Isorhamnetin was almost exclusively detected in the stamen extract, while the glucuronide conjugate (**83**) was mainly present in the sepal together with the glucuronide conjugates of kaempferol and quercetin (Fig. 7). As in the case of different galloylglucose and ellagitannin derivatives (see before), also within the flavonol derivatives the ionization efficiencies of differentially substituted conjugates may be different, and the observed differences in signals may be due to this, and not directly correspond to their abundancy in taken sample.

Several of the sugar derivatives of flavonols showed intriguing patterns of distribution among the floral organs. Two-sugar conjugates of kaempferol and quercetin had different distribution compared to other derivatives of the same aglycone. The dihexose derivatives of both flavonols (**64** and **24**, respectively) were present mainly in the stamen, whereas the malonylhexose derivatives (**85** and **75**, respectively) were detected mainly in the pistil (Fig. 7). On the other hand, the one-hexose derivative of kaempferol (**80**) detected had the same profile as for the glucuronide derivatives of kaempferol (**79**) and quercetin (**70**) (see above), while the one-hexose conjugate of quercetin (**72**) was merely observed in the reproductive organs, and was only detected in small amounts in the other organs petal, sepal and receptacle (Fig. 7).

The above observations suggest that different flavonols, as well as their different conjugates, play separate roles in floral organs. The unique patterns of individual sugar conjugates suggest different expression patterns of genes that encode enzymes catalyzing the synthesis of the different flavonols, as well as the ones responsible for attaching the various decorative moieties. For example, isorhamnetin was mainly found in the stamen, but in the sepal, where other flavonols were present as glucuronide conjugates, also isorhamnetin was similarly conjugated. A question then arises why the quercetin and kaempferol sugars are not malonylated in the stamens similarly to the derivatization of isorhamnetin. This suggests the presence of an enzyme with high substrate specificity to isorhamnetin in the stamens. Significant differences in the flavonoid composition among plants within the same family were recently reported in three *Compositae* plants (Lai et al., 2007). The versatility and exquisite substrate and site specificity of flavonoid modifying enzymes, as well as the divergent roles of different flavonoid derivatives in flowers or other plant organs, is a topic for investigation by several research teams (Vogt and Taylor, 1995; Miller et al., 1999; Jones et al., 2003; Luo et al., 2007).

3. Conclusions

In this study we performed non-targeted metabolic analysis of dissected strawberry floral organs. The approach used allowed the tentative identification and monitoring of more than a hundred secondary metabolites, most of them belonging to the phenolics class. The results demonstrate the immense variation in secondary metabolism existing between floral organs even in the case of metabolites with very similar structure. The current knowledge on the role of such metabolites or metabolite classes in flower organ physiology and development is very limited. Hence, this study should boost the efforts to understand the function/s of these intriguing molecules in the plant life cycle.

4. Experimental

4.1. Plant material and metabolite extraction

Strawberry (*Fragaria* × *ananassa* cv. Jonsok) plants were grown in the greenhouse under the following conditions: daylight 16 h, temperature 18–20 °C (night–day), and relative humidity 60–70%. To induce flowering, a 5–6 week short daylight period (13 h) was applied. Plants were grown in 12 cm pots in a peat-sand mixture (3:1) and fertilized weekly with Superex-9 (N 19%, P 5%, K 20%), supplied with micronutrients (Kekkilä, Finland). Strawberry flowers were collected at the day of full anthesis (Fig. 1), and the stamen, pistil, petal, sepal and receptacle (containing the immature achenes; Fig. 1) were separated and frozen immediately in liquid nitrogen. The separated organs of 15–20 flowers were pooled and ground to powder using a mixer mill (MM301, Retsch GmbH, Germany) for 2.5 min with the frequency of 30 s^{-1}. The frozen powder was weighed (the average weight of each pool of organs was: petals, 190 mg; sepals, 150 mg; stamens, 100 mg; pistils, 60 mg; receptacle, 200 mg) and methanol (80%) was added at a ratio of 1.5 ml to 500 mg powder for the metabolite extraction. The samples were vortexed, sonicated in a bath at room temperature (5510 Bransonic, Danbury, CT, USA) for 15 min, vortexed again, filtered (Acrodisc® 0.22 μm PTFE filter, PALL) and stored at −20 °C until analysed.

The samples were collected in the same manner from wild type strawberries and three transgenic lines as described in our related work on strawberry (Hanhineva et al., submitted for publication). In addition to separated organ samples, also samples from whole strawberry flowers were collected in five replicates from the four lines in order to conduct a non-targeted metabolite fingerprinting on the different lines (for metabolite analysis, see chapter UPLC-qTOF-MS analysis). To assess whether the different strawberry lines in the analysis were metabolically altered due to the gene transfer, Kruskal-Wallis nonparametric one-way analysis of variance was performed on the entire set of markers (i.e. mass signals) obtained from the samples of whole flowers by the MarkerLynx software. The resulting *p*-values were controlled for multiple hypotheses testing using a 5% false discovery rate (FDR) cutoff (Benjamini and Hochberg, 1995). The analysis showed that none of the markers had statistically significant differences between the lines. Thus, it was concluded that the gene transfer did not alter the metabolite profiles of the strawberry flowers, most likely because of very weak transgene expression in the floral organs, as determined in our related study (Hanhineva et al., submitted for publication). Therefore, in this analysis of the separated organs, the samples from each line (three transgenic lines and wild type; set of organ pools from each line) were regarded as four replicates in order to eliminate sample preparation or analysis related errors.

4.2. UPLC-qTOF-MS analysis

Metabolite analysis was carried out using a UPLC-PDA-qTOF-MS instrument (Waters Premier qTOF, Milford, MA, USA), with the UPLC column connected on-line to a PDA detector, and then to the MS detector. Separation of metabolites was performed using a 100 × 2.1 mm i.d., 1.7 μm UPLC BEH C18 column (Waters Acquity). The mobile phase consisted of 0.1% formic acid in acetonitrile:water (5:95, *v*/*v*) (phase A), and 0.1% formic acid in acetonitrile (phase B). The linear gradient program was as follows: 100–72% A over 22 min, 72–60% A over 0.5 min, 60–0% A over 0.5 min, held at 100% B for a further 1.5 min, then returned to the initial conditions (100% A) in 0.5 min, and conditioning at 100% A. The flow rate was 0.3 ml/min; column temperature was kept at 35 °C. The UV spectra (Waters Acquity PDA detector) were recorded between 210 and 500 nm, or the UV trace was measured at 240 nm (Waters Acquity UV detector). The wavelength resolution was 1.2 nm. Masses of the eluted compounds were detected by the Q-TOF equipped with electrospray ionization (ESI) source. Acquisition was performed in the ESI-positive and ESI-negative modes. The following settings were applied during the LC–MS runs: capillary voltage at 3.0 kV; cone voltage at 30 eV; collision energy at 3 eV and at 20 eV; argon was used as collision gas. For the LC–MS/MS analysis 20 eV collision was used. The *m*/*z* range was 50–1500 Da. The MS was calibrated using sodium formate, and leucine enkephalin was used as the lock mass. The injection volume of samples was 2 μl in the LC–MS analysis and 5 μl in the LC–MS/MS. A standard mixture containing 40 μg ml^{-1} of each of the following compounds: L-tryptophan, L-phenylalanine, *p*-coumaric acid, caffeic acid, sinapic acid, benzoic acid, quercetin dehydrate, kaempferol, rutin, and *trans*-resveratrol (all purchased from Sigma); naringenin, chlorogenic acid hemihydrate, *trans*-cinnamic acid and isorhamnetin (Fluka), ferulic acid (Aldrich) and tomatine (Apin chemicals) was used (5 μl injection volume) to monitor the quality of the chromatogram and reproducibility of the retention time throughout the runs and to aid in metabolite identification. The MassLynx software version 4.1 (Waters) was used to control all instruments and calculate the accurate masses.

4.3. Metabolomics data processing

The chromatograms obtained from UPLC-PDA-qTOF-MS analysis were processed by the MarkerLynx 4.1 software (Waters) for mass signal extraction and alignment, PCA analysis and creating a metabolite marker list. The data of mass peak intensities were collected using the following parameters: noise elimination level was set at 5.00, minimum peak intensity at 10, retention time window at 0.2; isotopic peaks were excluded and no internal standard was applied. The first 2 min of the chromatogram containing un-retained peaks and the last 3 min corresponding to column washing were excluded from the analysis. Since injections of samples in the positive and negative ionization modes were performed in the separate injection sets, MarkerLynx processing was done for each ionization mode independently. To facilitate the identification of the metabolites, a computer program implemented in MATLAB 7.3 was developed that groups the mass signals belonging to a single metabolite. The program accepts as an input the primary output of the MarkerLynx software run on the chromatographic data in both positive and negative modes. The algorithm used for the grouping of mass signals is comprised of two steps. First, based on a user-defined time shift the retention time values are synchronized between the positive and negative modes, in this analysis RT(ES−) = RT(ES+) + 0.02 min. Next, using a greedy clustering process, the mass signals in a joined list of both modes are grouped according to the similarity in their abundance profiles across different samples and according to the proximity in their retention time (using 0.08 s as the retention time threshold). Pearson correlation (with a threshold of 0.85) is used as the distance measure. Given the accuracy level (parts-per-million) as an input from the user, the program then identifies adducts and neutral loss ions, and detects parallel ions appearing in both ionization modes. The list of the neutral losses and adducts monitored is provided in Table 2. A similar approach for clustering together mass signals belonging to the same metabolite was described by Tautenhahn et al.(2007).

4.4. Metabolite identification

Information obtained from the computational processing was used as a starting point for the manual peak identification. First, metabolites that could be identified by standard compounds were verified by comparison of their R_t, UV/visible spectra and MS/MS fragmentation. Other metabolites were putatively assigned in the following four approaches: (a) The molecular formula suggested by the MassLynx software based on the accurate mass and isotopic pattern recognitions, was used for screening putative molecules from the Dictionary of Natural Products (Chapman & Hall/CRC) and the SciFinder Scholar databases (SciFinder Scholar™ 2007). In addition, information obtained from other sources including the KEGG (Kanehisa et al., 2006), KNApSAcK (Shinbo et al., 2006) and MoTo databases (Moco et al., 2006) was used. (b) The MS/MS fragmentation of the metabolites was compared with candidate molecules found in databases, and verified with earlier literature on similar compounds, especially when the presence of the metabolite was reported in strawberry. (c) Metabolites not included in the MS/MS analysis due to low intensity levels that did not allow MS/MS analysis were assigned based on in source fragmentation with high collision energy. Each mass spectrum was manually inspected by opening the reconstructed ion chromatograms and aligning the masses presumably originating from single metabolite, and verified by comparing to the clustered markers obtained from the computerized analysis. (d) In addition, UV/visible spectra was used in the identification whenever possible and calculated Log D values obtained from SciFinder (for pH 3 which is the pH of the UPLC mobile phase) were used for determining the degree of hydrophobicity of the metabolite (the higher the Log D, the more hydrophobic the compound is) and thus predicting the elution region in the chromatogram when compared to the Log D values of the standard compounds used.

4.5. Statistical analysis

The markers obtained from the MarkerLynx software were processed using a custom-made filtering statistical script written in MATLAB 7.0.4 (The MathWorks Inc.). MarkerLynx often misses the true value of mass signals in the data and marks them as zeros. Therefore, the first stage of the analysis was to distinguish between erroneously marked zero values and true "absent" calls. Three scenarios were considered, when examining the replicates for each of the markers: (a) The intensity is in the highest 90% of the overall data and there is one zero value out of four replicates. The zero value is removed from further analysis, and (b) the intensity is in the highest 90% and there are two or more zero values. A confident assignment of the marker levels for that group cannot be made. Therefore, the marker is excluded completely from the analysis, and (c) the mean intensity of non-zero values for the marker in the group is low. Therefore, the zeros are true calls and the zero values are replaced by the detection threshold of the instrument calculated from the overall distribution of the lowest values in the data.

Acknowledgements

AA is the incumbent of the Adolpho and Evelyn Blum Career Development Chair. The work in the Aharoni lab was supported by the William Z & Eda Bess Novick New Scientists Fund, the Israel Ministry of Science (IMOS Project #3-2552) and a research grant by the Henry S and Anne Reich Family Foundation. KH was funded by Jenny and Antti Wihuri Foundation and Tiura Agricultural Research Foundation. The personnel at the Research Garden of the University of Kuopio are warmly acknowledged for taking care of the strawberry plants. Arye Tishbee is thanked for operating the LC–MS instrument.

Appendix A. Supplementary data

Supplemental Table S1: Metabolites tentatively identified in the strawberry flowers and amounts detected as presented by the relative peak response area. The ion taken for area measurement is shown in the Table. Values are average of four lines with standard error. Supplementary data associated with this article can be found, in the online version, at doi:10.1016/j.phytochem.2008.07.009.

References

Aaby, K., Ekeberg, D., Skrede, G., 2007. Characterization of phenolic compounds in strawberry (*Fragaria* × *ananassa*) fruits by different HPLC detectors and contribution of individual compounds to total antioxidant capacity. J. Agric. Food Chem. 55, 4395–4406.

Aharoni, A., Keizer, L.C., Bouwmeester, H.J., Sun, Z., Alvarez-Huerta, M., Verhoeven, H.A., Blaas, J., van Houwelingen, A.M., de Vos, C.H.R., van der Voet, H., Jansen, R.C., Guis, M., Mol, J., Davis, R.W., Schema, M., van Tunen, A.J., O'Connel, A.P., 2000. Identification of the SAAT gene involved in strawberry flavor biogenesis by use of DNA microarrays. Plant Cell 12, 647–662.

Aharoni, A., deVos, C.H.R., Verhoeven, H.A., Maliepaard, C.A., Kruppa, G., Bino, R., Goodenowe, D.B., 2002. Nontargeted metabolome analysis by use of Fourier transform ion cyclotron mass spectrometry. Omics 6, 217–234.

Aharoni, A., Jongsma, M.A., Bouwmeester, H.J., 2005. Volatile science? Metabolic engineering of terpenoids in plants. Trends Plant. Sci. 12, 594–602.

Ardenghi, J.V., Kanegusuku, M., Niero, R., Filho, V.C., Monache, F.D., Yunes, R.A., De Souza, M.M., 2006. Analysis of the mechanism of antinociceptive action of niga-ichigoside F1 obtained from *Rubus imperialis* (Rosaceae). J. Pharm. Pharmacol. 58, 1669–1675.

Benjamini, Y., Hochberg, Y., 1995. Controlling the false discovery rate: a practical and powerful approach to multiple testing. J. Royal Stat. Soc. B 57, 289–300.

Cai, Y.Z., Xing, J., Sun, M., Zhan, Z.Q., Corke, H., 2005. Phenolic antioxidants (hydrolysable tannins, flavonoids and anthocyanins) identified by LC-ESI-MS and MALDI-QIT-TOF MS from *Rosa chinensis* flowers. J. Agric. Food Chem. 53, 9940–9948.

Clifford, M.N., Zheng, W., Kuhnert, N., 2006. Profiling the chlorogenic acids of aster by HPLC-MS^n. Phytochem. Anal. 17, 384–393.

Coen, E.S., Meyerowitz, E.M., 1991. The war of the whorls: genetic interactions controlling flower development. Nature 353, 31–37.

Cuyckens, F., Claeys, M., 2005. Determination of the glycosylation site in flavonoid mono-O-glycosides by collision induced dissociation of electrospray-generated deprotonated and sodiated molecules. J. Mass Spectrom. 40, 364–372.

Dixon, R.A., Xie, D.-Y., Sharma, S.B., 2005. Proanthocyanidins – a final frontier in flavonoid research? New Phytol. 165, 9–28.

Escobar-Restrepo, J.-M., Huck, N., Kessler, S., Gagliardini, V., Gheyselinck, J., Yang, W.-C., Grossniklaus, U., 2007. The FERONIA receptor-like kinase mediates male–female interactions during pollen tube reception. Science 317, 656–660.

Facchini, P.J., Hagel, J., Zulak, K.G., 2002. Hydroxycinnamic acid amide metabolism: physiology and biochemistry. Can. J. Bot. 80, 577–589.

Fait, A., Hanhineva, K., Beleggia, R., Dai, N., Rogachev, I., Nikiforova, V., Fernie, A.R., Aharoni, A., 2008. Reconfiguration of the achene and receptacle metabolic networks during strawberry fruit development. Plant Phys., in press.

Fukui, Y., Tanaka, Y., Kusumi, T., Iwashita, T., Nomoto, K., 2003. A rationale for the shift in colour towards blue in transgenic carnation flowers expressing the flavonoid 3′,5′-hydroxylase gene. Phytochemistry 63, 15–23.

Groteweld, E., 2006. The Science of Flavonoids. Springer Verlag, New York.

Gu, L., Kelm, M.A., Hammerstone, J.F., Beecher, G., Holden, J., Haytowitz, D., Prior, R.L., 2003. Screening of foods containing proanthocyanidins and their structural characterization using LC–MS/MS and thiolytic degradation. J. Agric. Food Chem. 51, 7513–7521.

Guo, S., Kenne, L., Lundgren, L.L., Rönnberg, B., Sundquist, B.G., 1998. Triterpenoid saponins from *Quillaja saponaria*. Phytochemistry 48, 175–180.

Halbwirth, H., Puhl, I., Haas, U., Jezik, K., Treutter, D., Stich, K., 2006. Two-phase flavonoid formation in developing strawberry (*Fragaria* × *ananassa*) fruit. J. Agric. Food Chem. 54, 1479–1485.

Hanhineva, K., Siljanen, H., Kokko, H., Rogachev, I., Aharoni, A., Kärenlampi, S., submitted for publication. Leaf metabolite profiling of strawberry (*Fragaria* × *ananassa*) transformed with stilbene synthase gene from frost grape (*Vitis riparia*).

Hashidoko, Y., 1996. The phytochemistry of *Rosa rugosa*. Phytochemistry 43, 535–549.

Heur, Y.H., Zeng, W., Stoner, G.D., 1992. Synthesis of ellagic acid O-alkyl derivatives and isolation of ellagic acid as a tetrahexanoyl derivative from *Fragaria* × *ananassa*. J. Nat. Prod. 55, 1402–1407.

Hu, W., Wang, Y., Bowers, C., Ma, H., 2003. Isolation, sequence analysis, and expression studies of florally expressed cDNAs in *Arabidopsis*. Plant Mol. Biol. 53, 545–563.

Huhman, D.V., Sumner, L.W., 2002. Metabolic profiling of saponins in Medicago sativa and Medicago truncatula using HPLC coupled to an electrospray ion-trap mass spectrometer. Phytochemistry 59, 347–360.

Hukkanen, A.T., Kokko, H.I., Buchala, A.J., McDougall, G.J., Stewart, D., Kärenlampi, S.O., Karjalainen, R.O., 2007. Benzothiadiazole induces the accumulation of phenolics and improves resistance to powdery mildew in strawberries. J. Agric. Food Chem. 55, 1862–1870.

Ingrouille, M., 2001. Sepals. In: Encyclopedia of Life Sciences. John Wiley & Sons, Ltd, Chichester. <http://www.els.net>.

Ingrouille, M., 2002. Flowers. In: Encyclopedia of Life Sciences. John Wiley & Sons, Ltd, Chichester. <http://www.els.net>.

Ishimaru, K., Omoto, T., Asai, I., Ezaki, K., Shimomura, K., 1995. Taxifolin 3-arabinoside from *Fragaria* × *ananassa*. Phytochemistry 40, 345–347.

Johnson, M.A., Preuss, D., 2002. Plotting a course: multiple signals guide pollen tubes to their targets. Dev. Cell. 2, 273–281.

Jones, P., Messner, B., Nakajima, J.-I., Schäffner, A.R., Saito, K., 2003. UGT73C6 and UGT78D1, glycosyltransferases involved in flavonol glycoside biosynthesis in Arabidopsis thaliana. J. Biol. Chem. 278, 43910–43918.

Kanegusuku, M., Sbors, D., Bastos, E.S., de Souza, M.M., Cechinil-Filho, V., Yunes, R.A., Monache, F.D., Niero, R., 2007. Phytochemical and analgesic activity of extract, fractions and a 19-Hydroxyursane-type triterpenoid obtained from *Rubus rosaefolius* (Rosaceae). Biol. Pharm. Bull. 30, 999–1002.

Kanehisa, M., Goto, S., Hattori, M., Aoki-Kinoshita, K.F., Itoh, M., Kawashima, S., Katayama, T., Araki, M., Hirakawa, M., 2006. From genomics to chemical genomics: new developments in KEGG. Nucleic Acid Res. 34, D354–D357.

Koponen, J.M., Happonen, A.M., Mattila, P.H., Törrönen, R., 2007. Contents of anthocyanins and ellagitannins in selected foods consumed in Finland. J. Agric. Food Chem. 55, 1612–1619.

Kumar, A., Altabella, T., Taylor, M.A., Tiburcio, A.F., 1997. Recent advances in polyamine research. Trends Plant Sci. 2, 124–130.

Kuo, P.L., Hsu, Y.L., Lin, T.C., Tzeng, W.S., Chen, Y.Y., Lin, C.C., 2007. Rugosin E, an ellagitannin, inhibits MDA-MB-231 human breast cancer cell proliferation and induces apoptosis by inhibiting nuclear factor-kappaB signaling pathway. Cancer Lett. 248, 280–291.

Kwak, M.S., Min, S.R., Lee, S.M., Kim, K.N., Liu, J.R., Paek, K.H., Shin, J.S., Bae, J.M., 2007. A sepal-expressed ADP-glucose pyrophosphorylase gene (*NtAGP*) is required for petal expansion growth in 'Xanthi' tobacco. Plant Physiol. 145, 277–289.

Kähkönen, M.P., Hopia, A.I., Heinonen, M., 2001. Berry phenolics and their antioxidant activity. J. Agric. Food Chem. 49, 4076–4082.

Lai, J.-P., Lim, Y.H., Su, J., Shen, H.-M., Ong, C.N., 2007. Identification and characterization of major flavonoids and caffeoylquinic acids in three compositae plants by LC/DAD-APCI/MS. J. Chromatogr. B 848, 215–225.

Laitinen, R.A.E., Immanen, J., Auvinen, P., Rudd, S., Alatalo, E., Paulin, L., Ainasoja, M., Kotilainen, M., Koskela, S., Teeri, T.H., Elomaa, P., 2005. Analysis of the floral transcriptome uncovers new regulators of organ determination and gene families related to flower organ differentiation in *Gerbera hybrida* (Asteraceae). Genome Res. 15, 475–486.

Laphookhieo, S., Karalai, C., Ponglimanont, C., 2004. New sesquiterpenoid and triterpenoids from the fruits of Rhizophora mucronata. Chem. Pharm. Bull. (Tokyo) 52, 883–885.

Li, X., Xiong, Z., Ying, X., Cui, L., Zhu, W., Li, F., 2006. A rapid ultra-performance liquid chromatography-electrospray ionization tandem mass spectrometric method for the qualitative and quantitative analysis of the constituents of the flower of *Trollius ledibouri* reichb. Anal. Chim. Acta 580, 170–180.

Lien, T.P., Kamperdick, C., Sung, T.V., Adam, G., 1999. Triterpenes from *Rubus cochinchinensis*. Phytochemistry 50, 463–465.

Luo, J., Nishiyama, Y., Fuell, C., Taguchi, G., Elliott, K., Hill, L., Tanaka, Y., Kitayama, M., Yamazaki, M., Bailey, P., Parr, A., Michael, A.J., Saito, K., Martin, C., 2007. Convergent evolution in the BAHD family of acyl transferases: identification and characterization of anthocyanin acyl transferases from *Arabidopsis thaliana*. Plant J. 50, 678–695.

Lunkenbein, S., Bellido, M.L., Aharoni, A., Salentijn, E.M.J., Kaldenhoff, R., Coiner, H.A., Muñoz-Blanco, J., Schwab, W., 2006. Cinnamate metabolism in ripening fruit. Characterization of a UDP-glucose:cinnamate glucosyltransferase from strawberry. Plant Physiol. 140, 1047–1058.

Madl, T., Sterk, H., Mittelbach, M., 2006. Tandem mass spectrometric analysis of a complex triterpene saponin mixture of *Chenopodium quinoa*. J. Am. Soc. Mass Spectrom. 17, 795–806.

Martin-Tanguy, J., 1997. Conjugated polyamines and reproductive development: Biochemical, molecular and physiological approaches. Physiol. Plant. 100, 675–688.

Mattila, P., Kumpulainen, J., 2002. Determination of free and total phenolic acids in plant-derived foods by HPLC with diode-array detection. J. Agric. Food Chem. 50, 3660–3667.

Meesapyodsuk, D., Balsevich, J., Reed, D.W., Covello, P.S., 2007. Saponin biosynthesis in Saponaria vaccaria. cDNAs encoding ß-amyrin synthase and a triterpene carboxylic acid glucosyltransferase. Plant Phys. 143, 959–969.

Mertens-Talcott, S.U., Jilma-Stohlawetz, P., Rios, J., Hinograni, L., Derendorf, H., 2006. Absorption, metabolism, and antioxidant effects of pomegranate (*Punica granatum* l.) polyphenols after ingestion of a standardized extract in healthy human volunteers. J. Agric. Food Chem. 23, 8956–8961.

Miller, K.D., Guyon, V., Evans, J.N., Shuttleworth, W.A., Taylor, L.P., 1999. Purification, cloning, and heterologous expression of a catalytically efficient flavonol 3-*O*-galactosyltransferase expressed in the male gametophyte of *Petunia hybrida*. J. Biol. Chem. 274, 34011–34019.

Mo, Y., Nagel, C., Taylor, L.P., 1992. Biochemical complementation of chalcone synthase mutants defines a role for flavonols in functional pollen. Proc. Natl. Acad. Sci. USA 89, 7213–7217.

Moco, S., Bino, R.J., Vorst, O., Verhoeven, H.A., de Groot, J., van Beek, T.A., Vervoort, J., de Vos, C.H.R., 2006. A liquid chromatography–mass spectrometry-based metabolome database for tomato. Plant Phys. 141, 1205–1218.

Mol, J., Cornish, E., Mason, J., Koes, R., 1999. Novel colored flowers. Curr. Opin. Biotechnol. 10, 198–201.

Moyano, E., Martinez-Garcia, J.F., Martin, C., 1996. Apparent redundancy in *myb* gene function provides gearing for the control of flavonoid biosynthesis in Antirrhinum flowers. Plant Cell 8, 1519–1532.

Mullen, W., McGinn, J., Lean, M.E., MacLean, M.R., Gardner, P., Duthie, G.G., Yokota, T., Crozier, A., 2002. Ellagitannins, flavonoids, and other phenolics in red raspberries and their contribution to antioxidant capacity and vasorelaxation properties. J. Agric. Food Chem. 50, 5191–5196.

Mullen, W., Yokota, T., Lean, M.E.J., Crozier, A., 2003. Analysis of ellagitannins and conjugates of ellagic acid and quercetin in raspberry fruits by LC–MS^n. Phytochemistry 64, 617–624.

Määttä, K.R., Kamal-Eldin, A., Törrönen, A.R., 2003. High-performance liquid chromatography (HPLC) analysis of phenolic compounds in berries with diode array and electrospray ionization mass spectrometric (MS) detection: ribes species. J. Agric. Food Chem. 51, 6736–6744.

Määttä-Riihinen, K.R., Kamal-Eldin, A., Törrönen, R., 2004. Identification and quantification of phenolic compounds in berries of *Fragaria* and *Rubus* species (family Rosaceae). J. Agric. Food Chem. 52, 6178–6187.

Nam, J.H., Jung, H.J., Choi, J., Lee, K.T., Park, H.J., 2006. The anti-gastropathic and anti-rheumatic effect of Niga-ichigoside F(1) and 23-hydroxytormentic acid isolated from the unripe fruits of *Rubus coreanus* in a rat model. Biol. Pharm. Bull. 29, 967–970.

Nielsen, A.H., Olsen, C.E., Møller, B.L., 2005. Flavonoids in flowers of 16 *Kalanchoe blossfeldiana* varieties. Phytochemistry 66, 2829–2835.

Niemetz, R., Gross, G.G., 2005. Enzymology of gallotannin and ellagitannin biosynthesis. Phytochemistry 66, 2001–2011.

Nunez, V., Gomez-Cordoves, C., Bartolome, B., Hong, Y-J., Mitchell, A.E., 2006. Non-galloylated and galloylated proanthocyanidin oligomers in grape seeds from *Vitus vinifera* L. cv. graciano, tempranillo and cabernet sauvignon. J. Sci. Food Agric. 86, 915–921.

Okuda, T., Yoshida, T., Hatano, T., Iwasaki, M., Kubo, M., Orime, T., Yoshizaki, M., Naruhashi, N., 1992. Hydrolysable tannins as chemotaxonomic markers in the rosaceae. Phytochemistry 31, 3091–3096.

Osbourn, A.E., 2003. Saponins in cereals. Phytochemistry 62, 1–4.

Palanivelu, R., Brass, L., Edlund, A.F., Preuss, D., 2003. Pollen tube growth and guidance is regulated by *POP2*, an Arabidopsis gene that controls GABA levels. Cell 114, 47–59.

Petsalo, A., Jalonen, J., Tolonen, A., 2006. Identification of flavonoids of *Rhodiola rosea* by liquid chromatography-tandem mass spectrometry. J. Chromatogr. A 1112, 224–231.

Pichersky, E., Raguso, R.A., Lewinshon, E., Croteau, R., 1994. Floral scent production in *Clarkia* (Onagraceae). Plant Phys. 106, 1533–1540.

Pichersky, E., Dudareva, N., 2007. Scent engineering: toward the goal of controlling how flowers smell. Trends Biotechnol. 25, 105–110.

Poter, L.J., 1994. Flavans and proanthocyanidins. In: Harbone, J.B. (Ed.), The Flavonoids. Advances in Research Since 1986. Chapman & Hall Ltd, New York, pp. 23–55.

Rommel, A., Wrolstad, R.E., 1993. Composition of flavonols in red raspberry juice as influenced by cultivar, processing, and environmental factors. J. Agric. Food Chem. 41, 1941–1950.

Ross, H.A., McDougall, G.J., Stewart, D., 2007. Antiproliferative activity is predominantly associated with ellagitannins in raspberry extracts. Phytochemistry 68, 218–228.

Santos-Buelga, C., Scalbert, A., 2000. Proanthocyanidins and tannin-like compounds: nature, occurrence, dietary intake, and effects on nutrition and health. J. Sci. Food Agric. 80, 1094–1117.

Shen, T., Wan, W., Yuan, H., Kong, F., Guo, H., Fan, P., Lou, H., 2007. Secondary metabolites from *Commiphora opobalsamum* and their antiproliferative effect on human prostate cancer cells. Phytochemistry 68, 1331–1337.

Schuurink, R.C., Haring, M.A., Clark, D.G., 2006. Regulation of volatile benzenoid biosynthesis in petunia flowers. Trends Plant Sci. 11, 20–25.

Seeram, N.P., Adams, L.S., Zhang, Y., Lee, R., Sand, D., Scheuller, H.S., Heber, D., 2006. Blackberry, black raspberry, and strawberry extracts inhibit growth and stimulate apoptosis of human cancer cells *in vitro*. J. Agric. Food Chem. 54, 9329–9339.

Seeram, N.P., Aronson, W.J., Zhang, Y., Henning, S.M., Moro, A., Lee, R.P., Sartippour, M., Harris, D.M., Rettig, M., Suchard, M.A., Pantuck, A.J., Belldegrun, A., Heber, D., 2007. Pomegranate ellagitannin-derived metabolites inhibit prostate cancer growth and localize to the mouse prostate gland. J. Agric. Food Chem. 55, 7732–7737.

Shinbo, Y., Nakamura, Y., Altaf-Ul-Amin, M., Asahi, H., Kurokawa, K., Arita, M., Saito, K., Ohta, D., Shibata, D., Kanaya, S., 2006. KNApSAcK: a comprehensive species-metabolite relationship database. In: Saito, K., Dixon, R.A., Willmitzer, L. (Eds.), Biotechnology in Agriculture and Forestry, Plant Metabolomics, vol.57, pp.165–181.

Sood, S., Nagar, P.K., 2004. Changes in endogenous polyamines during flower development in two diverse species of rose. Plant Growth Regul. 44, 117–123.

Sparg, S.G., Light, M.E., van Staden, J., 2004. Biological activities and distribution of plant saponins. J. Ethnopharmacol. 94, 219–243.

Spitaler, R., Schlorhaufer, P.D., Ellmerer, E.P., Merfort, I., Bortenschlager, S., Stuppner, H., Zidorn, C., 2006. Altitudinal variation of secondary metabolite profiles in flowering heads of Arnica Montana cv. ARBO. Phytochemistry 67, 409–417.

Starck, D., Eilert, U., Wray, V., Wolff, J., Jaggy, H., 1990. Tricoumaroylspermidine in flowers of Rosaceae. Phytochemistry 29, 2893–2896.

Tarenghi, E., Martin-Tanguy, J., 1995. Polyamines, floral induction and floral development of strawberry (*Fragaria ananassa* Duch.). Plant Growth Regul. 17, 157–165.

Tautenhahn, R., Böttcher, C., Neumann, S., 2007. Annotation of LC/ESI-MS mass signals. In: Proceedings of BIRD 2007 – First International Conference on Bioinformatics Research and Development. Springer LNBI 4414.

Tsukamoto, S., Tomise, K., Aburatani, M., Onuki, H., Hirorta, H., Ishiharajima, E., Ohta, T., 2004. Isolation of Cytochrome P450 inhibitors from strawberry fruit, *Fragaria* × *ananassa*. J. Nat. Prod. 67, 1839–1841.

Ukiya, M., Akihisa, T., Yasukawa, K., Tokuda, H., Suzuki, T., Kimura, Y., 2006. Anti-inflammatory, anti-tumor-promoting, and cytotoxic activities of constituents of marigold (*Calendula officinalis*) flowers. J. Nat. Prod. 69, 1692–1696.

Van der Krol, A., Chua, N.H., 1993. Flower development in petunia. Plant Cell 5, 1195–1203.

Van Schie, C.C.N., Haring, M.A., Schuurink, R.C., 2006. Regulation of terpenoid and benzenoid production in flowers. Curr. Opin. Plant Biol. 9, 203–208.

Vogt, T., Taylor, L.P., 1995. Flavonol 3-O-glycosyltransferases associated with petunia pollen produce gametophyte-specific flavonol diglycosides. Plant Physiol. 108, 903–911.

Weigel, D., 1998. From floral induction to floral shape. Curr. Opin. Plant Biol. 1, 55–59.

Wellmer, F., Riechmann, J.L., Alves-Ferreira, M., Meyerowitz, E.M., 2004. Genome-wide analysis of spatial gene expression in *Arabidopsis* flowers. Plant Cell 16, 1314–1326.

Wellmer, F., Alves-Ferreira, M., Dubois, A., Riechmann, J.L., Meyerowitz, E.M., 2006. Genome-wide analysis of gene expression during early *Arabidopsis* flower development. PLoS Genet. 2, e117.

Werner, C., Hu, W., Lorenzi-Riatsch, A., Hesse, M., 1995. Di-coumaroylspermidines and tri-coumaroylspermidines in anthers of different species of the genus Aphelandra. Phytochemistry 40, 461–465.

Winkel-Shirley, B., 2001. Flavonoid biosynthesis. A colorful model for genetics, biochemistry, cell biology, and biotechnology. Plant Physiol. 126, 485–493.

Wolters-Arts, M., Lush, W.M., Mariani, C., 1998. Lipids are required for directional pollen tube growth. Nature 392, 818–821.

Ylstra, B., Busscher, J., Franken, J., Hollman, P.C.H., Mol, J.N.M., vanTunen, A.J., 1994. Flavonols and fertilization in Petunia hybrida: localization and mode of action during pollen tube growth. Plant J. 6, 201–212.

Yu, Y.M., Chang, W.C., Wu, C.H., Chiang, S.Y., 2005. Reduction of oxidative stress and apoptosis in hyperlipidemic rabbits by ellagic acid. J. Nutr. Biochem. 16, 675–681.

Zabetakis, I., Holden, M.A., 1997. Strawberry flavour: analysis and biosynthesis. J. Sci. Food Agric. 74, 421–434.